Optimization of Scalable Broadcast for a Large Number of Antennas

Seok-Ho Chang, *Member, IEEE*, Jihwan P. Choi, *Member, IEEE*, Pamela C. Cosman, *Fellow, IEEE*, and Laurence B. Milstein, *Fellow, IEEE*

***Abstract*—In this paper, for a system incorporating a large number of antennas, we address the optimal space–time coding of multimedia scalable sources, which require unequal target error rates in their bitstream. First, in terms of the number of antennas, we analyze the behavior of the crossover point of the outage probability curves for the vertical Bell Laboratories space–time (V-BLAST) architecture with a linear or a maximum-likelihood receiver, and orthogonal space–time block codes (OSTBCs). We prove that, as the number of antennas increases with the transmission data rate fixed, the crossover point in outage probability monotonically decreases. This holds for any data rate employed by the system and is valid over propagation channels such as spatially correlated Rayleigh or Rician fading channels, as well as independent and identically distributed Rayleigh channels. We next show that, over such propagation channels with a large number of antennas, those analytical results can be used to simplify the computational complexity involved with the optimal space–time coding of a sequence of scalable packets, with no performance degradation.**

***Index Terms*—Diversity–multiplexing tradeoff (DMT), maximum-likelihood (ML) receiver, minimum mean square error (MMSE) receiver, multimedia scalable sources, multiple-input–multiple-output (MIMO) systems, orthogonal space–time block codes (OSTBC), outage probability, Rician channel, spatially correlated Rayleigh channel, vertical Bell Laboratories layered space–time (V-BLAST) architecture, zero-forcing (ZF) receiver.**

I. Introduction

The cross-layer optimization of wireless multimedia communications [1]–[3] has been motivated by the increasing demand for mobile multimedia services. Multimedia scalable sources, such as embedded images or scalable video [4]–[7], have a feature that the quality of the decoded source improves when the number of successfully received bits increases. Such advances in source codecs, however, have made the source bitstreams very susceptible to the impairments of mobile fading channels.

Multiple-input–multiple-output (MIMO) channels offer large gains in terms of link reliability and data rate. MIMO systems can be embodied in different ways to provide either a diversity gain or a spectral efficiency gain. Spatial diversity schemes, such as orthogonal space–time block codes (OSTBCs) [8], [9], extract diversity gain to combat signal fading from the channels and obtain reliability. The OSTBC is an important class of the space–time block code, in that it achieves the full diversity of channels with a very simple linear receiver. Spatial multiplexing schemes use a layered approach to increase capacity [10], [11]. One popular example is the vertical Bell Laboratories layered space–time (V-BLAST) architecture, where independent data signals are transmitted over antennas to increase the data rate, but full spatial diversity is usually not achieved.

Recently, with the exploration of high-frequency microwave waveforms and the progress in very large scale integration technology, a larger number of antennas can be incorporated in a MIMO system than before [12]. In this paper, we study the optimal design of such a MIMO system with a large number of antennas, for the transmission of multimedia scalable sources over spatially correlated Rayleigh or Rician fading channels. We first compare the outage probability performances of V-BLAST, using either a linear or a maximum-likelihood (ML) receiver, with OSTBC in terms of the number of antennas. The spatial correlation of MIMO channels tends to increase if more antennas are incorporated in the limited amount of space (i.e., if the antenna separation diminishes) [13], [14]. In such spatially correlated channels, OSTBC exhibits much less performance degradation than does V-BLAST [15], [16], that is, the performance of OSTBC becomes comparable with that of V-BLAST. To compare the outage probabilities of V-BLAST and OSTBC, we exploit the diversity–multiplexing tradeoff (DMT) [17], which is a standard tool in the characterization of the performance of space–time codes, in slowly varying fading channels in the high signal-to-noise ratio (SNR) regime.

Using the outage probability expression of a space–time code in [18], which is derived from the given DMT function, we analyze how the crossover point of the outage probability curves of V-BLAST and OSTBC behaves in the high-SNR regime, as a function of the number of antennas. Note that if the number of transmit or receive antennas changes, the amount of diversity or SNR gain, as well as the spatial multiplexing rate of the space–time codes, does not stay the same, and it is not clear how the crossover point behaves according to the effects of those

Manuscript received August 17, 2015; revised January 26, 2016; accepted March 8, 2016. Date of publication April 27, 2016; date of current version May 12, 2017. This research was supported in part by the "Cross-Ministry Giga KOREA Project" grant from the Ministry of Science, ICT and Future Planning, Korea, by the Army Research Office under Grant W911NF-14-1-0340, by the National Science Foundation under Grant CCF-1160832, by DGIST through the MIREBraiN program. The review of this paper was coordinated by Dr. S. Sun. *(Corresponding author: Jihwan P. Choi.)*

S.-H. Chang is with the Department of Computer Science and Engineering, Dankook University, Yongin 448-701, South Korea (e-mail: seokho@dankook.ac.kr).

J. P. Choi is with the Department of Information and Communications Engineering, Daegu Gyeongbuk Institute of Science and Technology, Daegu 711-873, South Korea (e-mail: jhchoi@dgist.ac.kr).

P. C. Cosman and L. B. Milstein are with the Department of Electrical and Computer Engineering, University of California at San Diego, La Jolla, CA 92093 USA (e-mail: pcosman@ucsd.edu; milstein@ece.ucsd.edu).

Color versions of one or more of the figures in this paper are available online at http://ieeexplore.ieee.org.

Digital Object Identifier 10.1109/TVT.2016.2558627

combined factors. We prove that, as the number of antennas increases with the transmission data rate fixed, the crossover point in outage probability monotonically decreases. The results are proven for any data rate employed by the space–time codes; furthermore, the results are valid in propagation channels such as spatially correlated Rayleigh or Rician fading channels, in addition to independent and identically distributed (i.i.d.) Rayleigh fading channels. In some literature, the crossover point of the ergodic capacity curves is investigated [19], [20]. In [18], the behavior of the crossover point of the error probabilities with regard to spectral efficiency was analyzed. However, we are unaware of any work that analytically compares the error probabilities of the space–time codes in terms of the number of transmit and receive antennas.

Because scalable sources have steadily decreasing importance for bits later in the stream, the error probability of an earlier packet should be lower than or equal to that of a later packet. Hence, when a scalable source is transmitted over MIMO channels and each packet of the source stream can be encoded with a different space–time code, the tradeoff between the space–time codes under consideration should be specified in terms of their target error rates. When a series of embedded images is transmitted, the optimization of space–time coding should be performed in a real-time manner depending on the rate–distortion characteristic of the specific image transmitted in each time slot. In particular, for a system with a large number of antennas, this real-time optimization is computationally complex, due to the complexity involved with V-BLAST decoding.

To address the matter, we exploit the behavior of the crossover point analyzed in terms of the number of antennas. That is, our analysis is used to optimally assign V-BLAST or OSTBC to each packet of the scalable bitstream to be transmitted over the correlated Rayleigh or Rician MIMO channels with a large number of antennas. With the suggested optimization strategy, the computational complexity involved with the optimization is exponentially simplified without losing any peak SNR (PSNR) performance, compared with the conventional exhaustive search. The rest of this paper is organized as follows. In Section II, we provide the system model and technical preliminaries. The analysis of the crossover point is provided in Section III. In Section IV, we present the optimization strategy for the space–time coding of scalable sources. In Section V, numerical results are provided, and we conclude this paper in Section VI.

II. Preliminaries

Consider a MIMO system with N_t transmit and N_r receive antennas. A space–time codeword $\mathbf{S} = [\mathbf{s}_1, \ldots, \mathbf{s}_T]$ of size $N_t \times T$ is transmitted over T symbol durations. The $N_r \times 1$ received signal vector $\mathbf{y}_k$ after matched filtering and sampling can be expressed as

$$\mathbf{y}_k = \mathbf{H}\mathbf{s}_k + \mathbf{n}_k, \tag{1}$$

where $\mathbf{s}_k$ is an $N_t \times 1$ transmitted signal vector, and $\mathbf{n}_k$ is an $N_r \times 1$ zero-mean complex additive white Gaussian noise vector with $\mathcal{E}[\mathbf{n}_k \mathbf{n}_l^H] = \sigma_n^2 \mathbf{I}_{N_r} \delta(k-l)$, where $(\cdot)^H$ denotes Hermitian operation. $\mathbf{H}$ denotes the $N_r \times N_t$ channel matrix, whose entry h_{ij} represents the complex channel gain between the jth transmit antenna and the ith receive antenna. The channel matrix can be modeled as [21]

$$\mathbf{H} = \sqrt{\frac{K}{K+1}}\bar{\mathbf{H}} + \sqrt{\frac{1}{K+1}}\mathbf{R}_r^{\frac{1}{2}}\,\mathbf{H}_{\mathbf{w}}\,\mathbf{R}_t^{\frac{1}{2}}, \tag{2}$$

where $K > 0$ is the Rician factor, and $\bar{\mathbf{H}}$ represents the channel matrix related to line-of-sight (LOS) signal components. The Frobenius norm of $\bar{\mathbf{H}}$ is normalized as $(N_r N_t)^{1/2}$, and $\bar{\mathbf{H}}$ is assumed to be known to both the transmitter and the receiver. $\mathbf{R}_t$ is an $N_t \times N_t$ transmit spatial correlation matrix, $\mathbf{R}_r$ is an $N_r \times N_r$ receive spatial correlation matrix, and $(\cdot)^{1/2}$ represents the Hermitian square root of a matrix. We use the exponential correlation model with $(\mathbf{R}_t)_{i,j} = \rho_t^{|i-j|}$ and $(\mathbf{R}_r)_{i,j} = \rho_r^{|i-j|}$, where $(\cdot)_{i,j}$ denotes the (i,j)th entry of a matrix; and ρ_t and ρ_r are the transmit and receive spatial correlation coefficients between adjacent antennas, respectively. In (2), $\mathbf{H}_{\mathbf{w}}$ is an $N_r \times N_t$ channel matrix whose entries are i.i.d. $\sim \mathcal{CN}(0,1)$, and $\mathbf{H}_{\mathbf{w}}$ is assumed to be known at the receiver, but not known at the transmitter (i.e., channel state information (CSI) is available only at the receiver). It is also assumed that $\mathbf{H}_{\mathbf{w}}$ is random, but constant over T symbol durations. Let γ_s denote the SNR per symbol, which is defined as $\gamma_s := \mathcal{E}[|(\mathbf{s}_k)_i|^2]/\sigma_n^2$, where $(\cdot)_i$ denotes the ith component of a vector. Let N_s denote the number of symbols packed within a space–time codeword $\mathbf{S} = [\mathbf{s}_1, \ldots, \mathbf{s}_T]$. Then, the spatial multiplexing rate of $\mathbf{S}$ is defined as N_s/T.

Next, we briefly present the outage probability expression of the space–time code, which is derived in [18], for any given piecewise-linear DMT function [17]. We let r and d denote the multiplexing and diversity gains defined in [17], respectively. We consider a space–time code whose DMT characteristic function is given by

$$d(r) = v - ur, \quad \text{for } \alpha \le r \le \beta \ (\alpha > 0), \tag{3}$$

where $d(r) \ge 0$, and $u \ge 0$ and $v \ge 0$ are real constants. Let $P_{\text{out}}(\gamma_s)$ denote the outage probability for the space–time code whose DMT is given by (3). In [18], it is shown that, as $\gamma_s \to \infty$, $P_{\text{out}}(\gamma_s)$ can be expressed as

$$P_{\text{out}}(\gamma_s) = k_d \left(\frac{2^R}{k_r}\right)^u \frac{1}{\gamma_s^v}, \quad \text{for } \left(\frac{2^R}{k_r}\right)^{\frac{1}{\beta}} \le \gamma_s \le \left(\frac{2^R}{k_r}\right)^{\frac{1}{\alpha}}, \tag{4}$$

where k_d is an arbitrary positive constant, R is the spectral efficiency (bits/s/Hz), and k_r is an arbitrary positive constant subject to the constraint that $2^R/k_r$ is greater than unity. Consider two space–time codes that have linear DMT characteristics as follows:

$$d_1(r) = v_1 - u_1 r \quad \text{and} \quad d_2(r) = v_2 - u_2 r, \quad \text{for } \alpha \le r \le \beta(\alpha > 0), \tag{5}$$

where

$$u_i > 0 \text{ and } v_i > 0 \quad (i = 1, 2), \tag{6}$$

$$v_1 - u_1\alpha < v_2 - u_2\alpha, \tag{7}$$

$$v_1 - u_1\beta > v_2 - u_2\beta. \tag{8}$$

That is, there exists a crossover in $\alpha < r < \beta$ for the two DMT functions. Let $P_{\mathrm{out},1}(\gamma_s)$ and $P_{\mathrm{out},2}(\gamma_s)$ denote the outage probabilities of the space–time codes whose DMT functions are given by $d_1(r)$ and $d_2(r)$, respectively. Then, from (4), as $\gamma_s \to \infty$, we have

$$P_{\mathrm{out},i}(\gamma_s) = k_d \left(\frac{2^R}{k_r}\right)^{u_i} \frac{1}{\gamma_s^{v_i}} \; (i = 1, 2), \tag{9}$$

for $(2^R/k_r)^{1/\beta} \le \gamma_s \le (2^R/k_r)^{1/\alpha}$. From (9), for a given spectral efficiency R, we find the outage probability P^*_{out}, for which $P_{\mathrm{out},1}(\gamma_s)$ and $P_{\mathrm{out},2}(\gamma_s)$ are identical. In [18], it is shown that the crossover point in outage probabilities P^*_{out} is given by

$$P^*_{\mathrm{out}} = k_d \left(\frac{2^R}{k_r}\right)^{\frac{u_1 v_2 - u_2 v_1}{v_2 - v_1}}. \tag{10}$$

Moreover, it is shown that

$$\begin{aligned} &P_{\mathrm{out},1}(\gamma_s) < P_{\mathrm{out},2}(\gamma_s), \quad \text{for} \left(\frac{2^R}{k_r}\right)^{\frac{1}{\beta}} \le \gamma_s < \gamma_s^*, \\ &P_{\mathrm{out},1}(\gamma_s) > P_{\mathrm{out},2}(\gamma_s), \quad \text{for } \gamma_s^* < \gamma_s \le \left(\frac{2^R}{k_r}\right)^{\frac{1}{\alpha}}, \end{aligned} \tag{11}$$

where γ_s^* is the crossover point in SNR, which corresponds to P^*_{out} in outage probability.

The DMT characteristics of V-BLAST, using either a minimum mean square error (MMSE) or a zero-forcing (ZF) linear receiver, with OSTBC, which are denoted by $d_V(r)$ and $d_O(r)$, respectively, are given by [22]

$$d_V(r) = \begin{cases} N_r - N_t + 1 - \frac{1}{N_t}(N_r - N_t + 1)r, & \\ & \text{for } 0 \le r \le N_t, \\ 0, & \text{for } N_t \le r < \infty, \end{cases} \tag{12}$$

$$d_O(r) = \begin{cases} N_r N_t - \frac{1}{r_s} N_r N_t \, r, & \text{for } 0 \le r \le r_s, \\ 0, & \text{for } r_s \le r < \infty, \end{cases} \tag{13}$$

where r_s denotes the spatial multiplexing rate of the OSTBC. For $N_t = 2$, the Alamouti scheme achieves $r_s = 1$. On the other hand, $r_s = 3/4$ is the maximum achievable rate for $N_t = 3$ or 4 in the complex OSTBC, and $r_s = 1/2$ is the maximum rate for $N_t > 4$ [23]. To compare the preceding codes, it is assumed that $N_r \ge N_t \ge 2$.

III. Behavior of Crossover Point for V-BLAST With a Linear Receiver and Orthogonal Space Time Block Codes in Terms of the Number of Antennas

Using (12) and (13), we set $d_1(r) = d_V(r)$ and $d_2(r) = d_O(r)$ in (5). From $N_t \ge 2$ and $r_s \le 1$, we have $r_s < N_t$. Thus, from (12) and (13), it is seen that, for the range of multiplexing gain, i.e., $0 < r \le r_s$, the condition of (6) is satisfied. Furthermore, from $N_r \ge N_t \ge 2$, it can be shown that

$$d_V(0) - d_O(0) = (N_r + 1)(1 - N_t) < 0, \tag{14}$$

$$d_V(r_s) - d_O(r_s) = (N_r - N_t + 1)(1 - r_s/N_t) > 0. \tag{15}$$

Eqs. (14) and (15) satisfy the conditions of (7) and (8), respectively, when setting $\alpha = \varepsilon$ and $\beta = r_s$, where $\varepsilon > 0$ denotes an arbitrarily small positive number. As a result, (11) holds, which indicates that, in $(2^R/k_r)^{1/r_s} \le \gamma_s < \infty$, there exists a crossover point of the outage probabilities for V-BLAST, using either an MMSE or a ZF linear receiver, with OSTBC. Furthermore, from (10), (12), and (13), it can be shown that the crossover point of the outage probabilities P^*_{out} is given by

$$P^*_{\mathrm{out}} = k_d \left(\frac{2^R}{k_r}\right)^{\frac{(N_r - N_t + 1)(1 - N_t/r_s)N_r}{(N_t - 1)(N_r + 1)}}. \tag{16}$$

In the following, we will investigate the behavior of P^*_{out} in terms of the number of antennas. If we let $N_t = N_r = n$ in (16), we have

$$P^*_{\mathrm{out}} = k_d \left(\frac{2^R}{k_r}\right)^{\frac{n - n^2/r_s}{n^2 - 1}}. \tag{17}$$

We will prove that P^*_{out}, given by (17), is a strictly decreasing function in n, under the condition that $n \ge 2$. We define function $f(n)$ as

$$f(n) = \frac{n - n^2/r_s}{n^2 - 1}. \tag{18}$$

Assuming that n is a real number, $df(n)/dn$ can be expressed as

$$\frac{df(n)}{dn} = \frac{-r_s n^2 + 2n - r_s}{r_s(n^2 - 1)^2}. \tag{19}$$

Let $g(n) = -r_s n^2 + 2n - r_s$ be the numerator of $df(n)/dn$. Then, it can be shown that $g(n)$ is a strictly decreasing function in n for $n \ge 1/r_s$. To begin, suppose that $n \ge 4$. Then, from the fact that $1/2 \le r_s \le 3/4$ (i.e., $4/3 \le 1/r_s \le 2$) for $N_t \ge 4$, we have

$$g(n) \le g(4) = -17 r_s + 8 < 0. \tag{20}$$

From (19) and (20), it follows that

$$\frac{df(n)}{dn} < 0, \quad \text{for } n \ge 4. \tag{21}$$

If we substitute $n = 2$, 3, and 4 along with the corresponding spatial multiplexing rates (i.e., $r_s = 1$ for $N_t = 2$ and $r_s = 3/4$ for $N_t = 3$ or 4) into (18), we have

$$f(2) = -2/3, \qquad f(3) = -9/8, \qquad f(4) = -52/45. \tag{22}$$

From (21) and the inequality of $f(2) > f(3) > f(4)$ in (22), it follows that $df(n)/dn < 0$ for $n \ge 2$. Thus, from (17), (18), and $k_d > 0$ and $2^R/k_r > 1$ given below (4), it is seen that P^*_{out} is a strictly decreasing function in n (≥ 2), regardless of the given spectral efficiency R. That is, as the number of antennas, i.e., $N_t = N_r$ (≥ 2), increases, the crossover point in the outage probability monotonically decreases for any fixed spectral efficiency. We note that, in the preceding analysis, the same spectral efficiency R is used for both V-BLAST and OSTBC. Furthermore, R stays the same when the number of antennas increases. Let $P^*_{\mathrm{out},1}$ denote the crossover point when

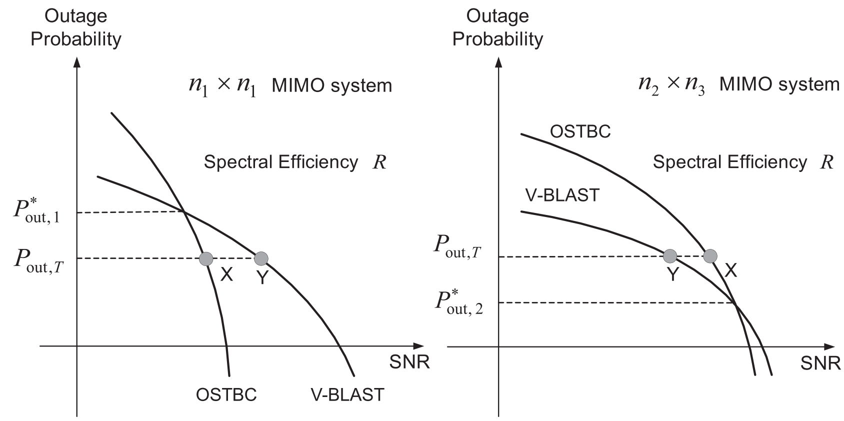

Fig. 1. Outage probabilities of V-BLAST with a linear receiver and OSTBC for the same given spectral efficiency of R. For the number of antennas $n_1 < n_2 \leq n_3$, the outage probabilities have the property of $P^*_{\text{out},1} > P^*_{\text{out},2}$. This figure can be also used to qualitatively depict the results, which are given in Appendix A, for V-BLAST with an ML receiver and OSTBC.

the number of antennas $N_t = N_r = n_1$ is employed, and let $P^*_{\text{out},2}$ denote the crossover point when $N_t = N_r = n_2$ is used. Then, from the results given earlier, we have

$$P^*_{\text{out},1} > P^*_{\text{out},2}, \qquad \text{for } n_1 < n_2. \tag{23}$$

We next analyze how the crossover point behaves as only the number of receive antennas N_r increases, for any given number of transmit antennas $N_t\ (\leq N_r)$. Substituting $N_r = m$ into (16), we have

$$P^*_{\text{out}} = k_d \left(\frac{2^R}{k_r}\right)^{\frac{(m-N_t+1)(1-N_t/r_s)m}{(N_t-1)(m+1)}}. \tag{24}$$

It will be shown that P^*_{out}, given by (24), is a strictly decreasing function in m, under the condition that $m \geq N_t \geq 2$. We define function $h(m)$ as

$$h(m) = \frac{(1 - N_t/r_s)}{N_t - 1} \cdot \frac{m(m - N_t + 1)}{m + 1}. \tag{25}$$

Let $p(m) = m(m - N_t + 1)/(m + 1)$ be the second factor of $h(m)$. If we assume that m is a real number, $dp(m)/dm$ can be expressed as

$$\frac{dp(m)}{dm} = \frac{m^2 + 2m - N_t + 1}{(m + 1)^2}. \tag{26}$$

If we let $q(m) = m^2 + 2m - N_t + 1$ be the numerator of $dp(m)/dm$, it can be shown that $q(m)$ is a monotonically increasing function in m for $m \geq 2$. From this and $m \geq N_t \geq 2$, $q(m)$ satisfies

$$q(m) \geq q(N_t) = N_t^2 + N_t + 1 > 0. \tag{27}$$

From (26) and (27), we have

$$\frac{dp(m)}{dm} > 0, \qquad \text{for } m \geq N_t. \tag{28}$$

Furthermore, from $N_t \geq 2$ and $1/2 \leq r_s \leq 1$, we have $(1 - N_t/r_s)(N_t - 1) < 0$. Hence, from (24), (25), (28), and $k_d > 0$ and $2^R/k_r > 1$ given in Section II, it follows that P^*_{out} is a strictly decreasing function in m, regardless of the given spectral efficiency R and the given number of transmit antennas N_t. In other words, for any fixed spectral efficiency and any fixed number of transmit antennas, as the number of receive antennas, i.e., $N_r\ (\geq N_t \geq 2)$, increases, the crossover point in the outage probability monotonically decreases.

Suppose that the number of transmit antennas N_t is fixed. Then, we let $P^*_{\text{out},1}$ denote the crossover point when the number of receive antennas $N_r = m_1 (\geq N_t)$ is used and let $P^*_{\text{out},2}$ denote the crossover point when $N_r = m_2 (\geq N_t)$ is used. Then, from the previous results, we have

$$P^*_{\text{out},1} > P^*_{\text{out},2}, \qquad \text{for } m_1 < m_2. \tag{29}$$

Recall that, as given by (23), when the number of antennas increases such that an $n_1 \times n_1$ system becomes an $n_2 \times n_2$ system $(n_1 < n_2)$, the crossover point in the outage probability monotonically decreases. In addition, as given by (29), when the number of antennas increases such that an $n_2 \times n_2$ system becomes an $n_2 \times n_3$ system $(n_2 < n_3)$, the crossover point also monotonically decreases. Based on these, the outage probabilities of V-BLAST with a linear receiver and OSTBC are qualitatively depicted in Fig. 1, where $P^*_{\text{out},1}$ denotes the crossover point for an $n_1 \times n_1$ MIMO system, and $P^*_{\text{out},2}$ is the crossover point for an $n_2 \times n_3$ MIMO system $(n_1 < n_2 \leq n_3)$. Suppose that a target outage probability $P_{\text{out},T}$ is smaller than $P^*_{\text{out},1}$ but greater than $P^*_{\text{out},2}$. Then, from Fig. 1, it is seen that OSTBC is preferable to V-BLAST for an $n_1 \times n_1$ system, whereas the latter is preferable to the former for an $n_2 \times n_3$ system. In Appendix A, we prove that the crossover point for V-BLAST with an ML receiver and OSTBC shows the same behavior as given by (23) and (29).

We note that DMT characteristics are not influenced by spatial correlation or LOS signal components at high SNR [24], [25]. In other words, the DMT function for spatially correlated Rayleigh or Rician fading is identical to that for i.i.d. Rayleigh fading. This is because, as described in [24], when the SNR approaches infinity, only the number of channel eigenmodes determines the performance. Spatial correlation or LOS components primarily affect the condition number of the channel matrix, and hence, the impact of such propagation on the performance is not observed at high SNR. This indicates that the analysis of the crossover points here is valid over correlated

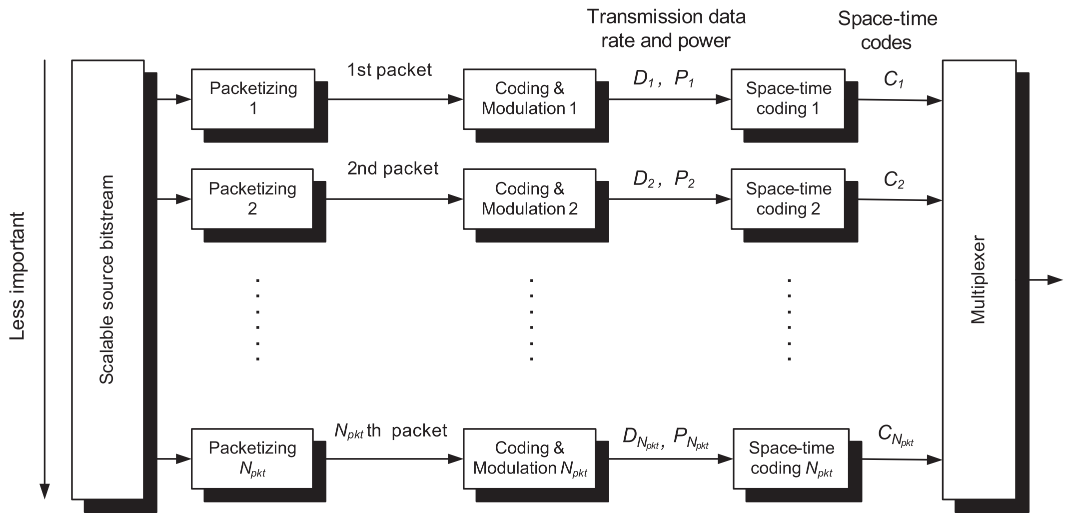

Fig. 2. Scalable source transmission system. D_i, P_i, and C_i denote the transmission data rate, power, and space–time code assigned to the ith packet, respectively $(1 \leq i \leq N_{\rm pkt})$.

Rayleigh or Rician channels and i.i.d. Rayleigh channels at high SNR.

IV. Optimal Space–Time Coding of Scalable Sources for a Large Number of Antennas

The analysis in Section III can be exploited to optimally design a MIMO system with a large number of antennas for the transmission of multimedia scalable sources. To begin, we briefly present the properties of scalable bitstreams described in [18, Sec. IV]. Scalable codecs adopt progressive transmission so that encoded data have gradual differences of importance in their bitstreams. Suppose that the system takes the bitstream from the scalable source encoder and transforms it into a sequence of $N_{\rm pkt}$ packets. Each of these $N_{\rm pkt}$ scalable packets can be encoded with different transmission data rates and powers, as well as different space–time codes, to achieve the best end-to-end performance measured by the expected distortion of the source. Such a system is depicted in Fig. 2. Note that the error probability of an earlier packet in a sequence of scalable packets should be lower than or equal to that of a later packet.

Let N_d and N_p denote the numbers of candidate transmission data rates and powers employed by a system, respectively. The numbers of possible assignments of N_d data rates and N_p powers to a sequence of $N_{\rm pkt}$ packets are $N_d^{N_{\rm pkt}}$ and $N_p^{N_{\rm pkt}}$, respectively, which exponentially grow as $N_{\rm pkt}$ increases. Furthermore, in a MIMO system, if each packet can be encoded with different space–time codes (e.g., V-BLAST or OSTBC), the assignment of space–time codes and data rates and powers to $N_{\rm pkt}$ packets yields a more complicated optimization problem. Note that each source, e.g., an image, has its inherent rate–distortion characteristic, from which the performance of the expected distortion is computed. For example, when a series of images is transmitted, the aforementioned optimization should be addressed in a real-time manner, considering which specific image (i.e., rate–distortion characteristic) is transmitted in the current time slot. To address this matter, for a single-input–single-output system, there have been many studies about the optimal assignment of data rates to a sequence of scalable packets [26]–[28].

On the other hand, for a MIMO system with a large number of antennas, we exploit the analysis in the previous section for the optimal assignment of space–time codes to a sequence of scalable packets. Suppose that the assignment of space–time codes in an $n_1 \times n_1$ MIMO system has been optimized, with the result that the kth packet $(1 \leq k \leq N_{\rm pkt})$, which has a data rate R_k, has been encoded with V-BLAST. Then, our analysis indicates that, in an $n_2 \times n_3$ MIMO system $(n_1 < n_2 \leq n_3)$, the aforementioned kth packet, which has data rate R_k, should be also encoded with V-BLAST rather than with OSTBC. This is because we have proven that, for a fixed data rate (i.e., spectral efficiency times signal bandwidth), as the number of antennas increases, the crossover point in the outage probability monotonically decreases. In other words, if V-BLAST is preferable for a packet in an $n_1 \times n_1$ system, then another packet with the same data rate in an $n_2 \times n_3$ system $(n_1 < n_2 \leq n_3)$ should be also encoded with V-BLAST, as long as the target error rates of the two packets are the same (see Fig. 1). Note that the target error rates of scalable packets depend on their application source (e.g., an embedded image with a specific rate–distortion characteristic) and their positions in the scalable bitstream, and that we evaluate the same application source, which is packetized in the same way, for both $n_1 \times n_1$ and $n_2 \times n_3$ systems.

Based on that, we further suppose that the k_1th,…,$k_{N_{\rm vb}}$th packets $(1 \leq k_1 < \cdots < k_{N_{\rm vb}} \leq N_{\rm pkt})$ have been encoded with V-BLAST as a result of the optimization for an $n_1 \times n_1$ system. Then, in an $n_2 \times n_3$ system, the aforementioned $N_{\rm vb}$ packets should be also encoded with V-BLAST, and only the remaining $N_{\rm pkt} - N_{\rm vb}$ packets need to be optimized for their space–time coding.

For the optimal assignment of space–time codes to $N_{\rm pkt}$ packets, the expected distortion of the source should be evaluated for each possible assignment. Note that each evaluation includes the decoding of the packets encoded with V-BLAST. An MMSE or a ZF linear receiver for V-BLAST incorporates an inversion operation of a channel matrix $\mathbf{H}$, and the amount of computation required for the inversion is in general $O(n^3)$,[1] where n is the size of the channel matrix in an $n \times n$ MIMO system. Thus, the computational complexity involved with the decoding of V-BLAST exponentially grows as the number of antennas increases, which indicates that the V-BLAST receiver will be highly complex for a large number of antennas. Note that the complexity of V-BLAST decoding for an $n_1 \times n_1$ system becomes insignificant compared with that for an $n_2 \times n_3$ system when n_1 is chosen such that it is sufficiently smaller than n_2. Based on the preceding statements, we propose an optimization strategy for the space–time coding of scalable sources in a MIMO system with a large number of antennas, as follows.

Step 1) Optimize the assignment of the space–time codes (i.e., OSTBC or V-BLAST) to a sequence of $N_{\rm pkt}$ scalable packets for an $n_1 \times n_1$ system, which is referred to as a *pilot system*.

Step 2) If the k_1th,…,$k_{N_{\rm vb}}$th packets $(1 \leq k_1 < \cdots < k_{N_{\rm vb}} \leq N_{\rm pkt})$ have been encoded with V-BLAST in Step 1, then assign V-BLAST to the same $N_{\rm vb}$ packets in an $n_2 \times n_3$ system $(n_1 < n_2 \leq n_3)$, which is referred to as a *target system*.

Step 3) Optimize the assignment of the space–time codes to the remaining $N_{\rm pkt} - N_{\rm vb}$ packets for a target system.

In Steps 1 and 3, we employ the same scalable source that is packetized identically. In addition, we use the same system parameters such as the sets of transmission data rates and powers assigned to a sequence of $N_{\rm pkt}$ packets.

Note that, in [18], it is assumed that a constant transmission power is used for a sequence of $N_{\rm pkt}$ scalable packets. Thus, with constant transmission power, the earlier packet requires a transmission data rate that is less than or equal to that of the later packet, to provide the unequal error protection of scalable packets. On the other hand, the work in this paper considers a more general case where unequal transmission powers are allowed for a sequence of scalable packets for the purpose of unequal error protection. As a result, the earlier packet does not necessarily have a data rate that is less than or equal to that of the later packet. Without any such assumptions, the number of possible assignments of two space–time codes (i.e., OSTBC and V-BLAST) to a sequence of $N_{\rm pkt}$ packets is $2^{N_{\rm pkt}}$.[2] It can be shown that, by exploiting the optimization results in a pilot system, the number of possible assignments of two space–time codes to $N_{\rm pkt}$ scalable packets is reduced from $2^{N_{\rm pkt}}$ to $2^{N_{\rm pkt}-N_{\rm vb}}$.

Finally, in the following, we present the message operation between the transmitter and the receiver required for the space–time coding of scalable packets, as depicted in Fig. 3.

[1]The use of Gaussian elimination is assumed [29].

[2]Note that this differs from $N_{\rm pkt} + 1$, which is derived in [18] based on the assumption that the earlier packet has a data rate that is less than or equal to that of the later packet.

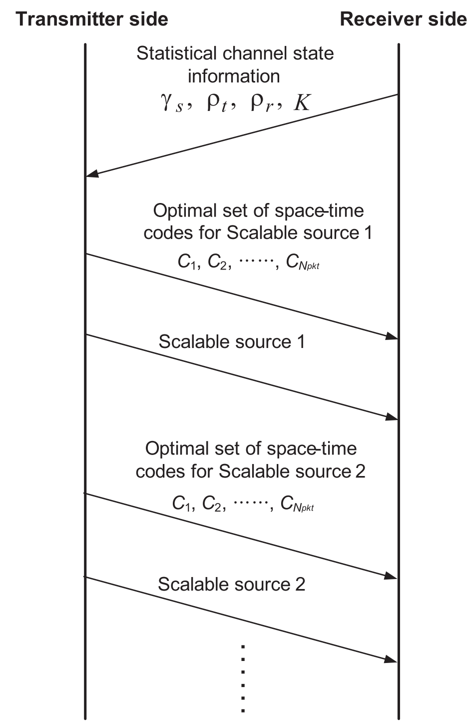

Fig. 3. Message protocol between the transmitter and the receiver required for the space–time coding of scalable packets.

Step 1) Statistical characteristics of the fading channel, such as average channel SNR, spatial correlation between antennas, and Rician factor, are estimated at the receiver side and fed back to the transmitter.

Step 2) At the transmitter side, based on the statistical CSI, the optimal set of space–time codes is found for the specific scalable source, which is to be transmitted in the current time slot. Recall that the steps of finding the optimal set were described earlier here.

Step 3) The scalable source is encoded by the optimal set of space–time codes found in Step 2 and is transmitted along with side information informing the receiver of the optimal set of codes.

Note that statistical CSI is a long-term characteristic of the channel, compared with the instantaneous CSI, such as instantaneous fading channel SNR. Thus, in Step 1, it is a natural assumption that its estimation is easier and does not have to be fed back to the transmitter frequently. In Step 3, the size of the message is $N_{\rm pkt}$ bits, since it indicates whether each of $N_{\rm pkt}$ packets is encoded by V-BLAST or OSTBC. As an example, for the transmission of a 512 × 512 embedded image with a rate of 1 bit per pixel (bpp), a sequence of 512 packets is considered in [27] (i.e., $N_{\rm pkt} = 512$). For this case, the size of the image is $512 \times 512 \times 1 = 262\,144$ bits, whereas the size of the message is 512 bits (i.e., the amount of overhead is $512/262\,144 = 0.195\%$).

V. Numerical Evaluation

First, we numerically evaluate the outage probabilities of V-BLAST with an MMSE receiver and OSTBC for various numbers of antennas.

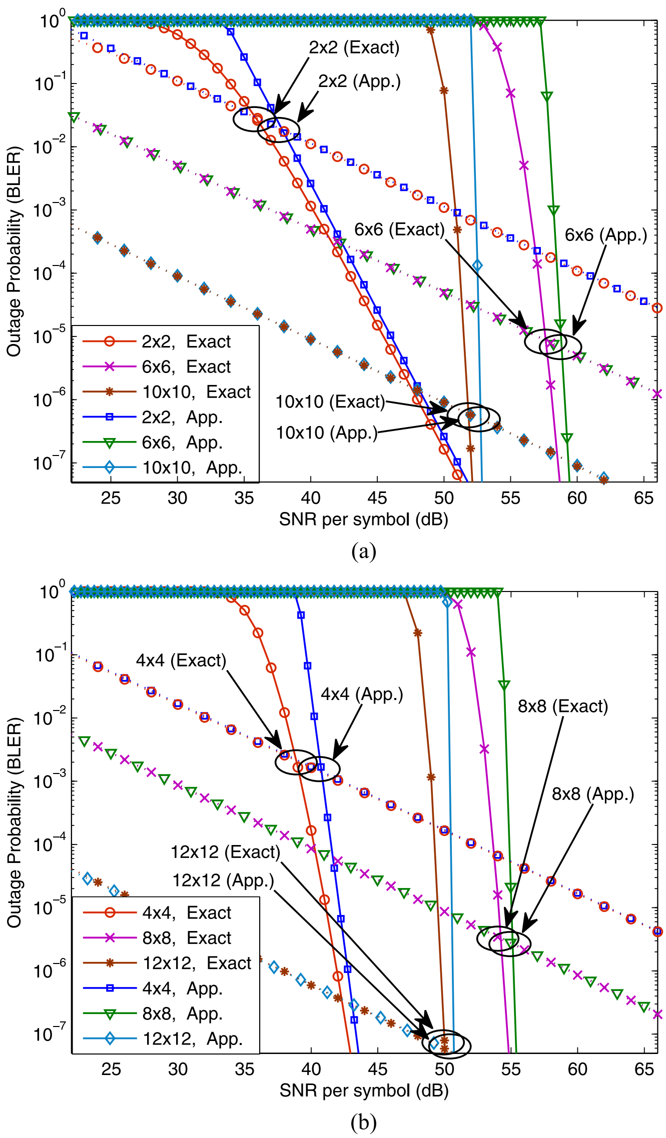

Fig. 4. Exact and high-SNR approximate outage probabilities for $R = 12$ bits/s/Hz in the spatially correlated Rayleigh fading channels with $\rho_t = \rho_r = 0.3$. Solid curves denote the outage probabilities of OSTBC, and dotted curves denote those of V-BLAST with an MMSE receiver. The crossover points of outage probabilities are marked with circles. (a) 2×2, 6×6, and 10×10 MIMO systems. (b) 4×4, 8×8, and 12×12 MIMO systems.

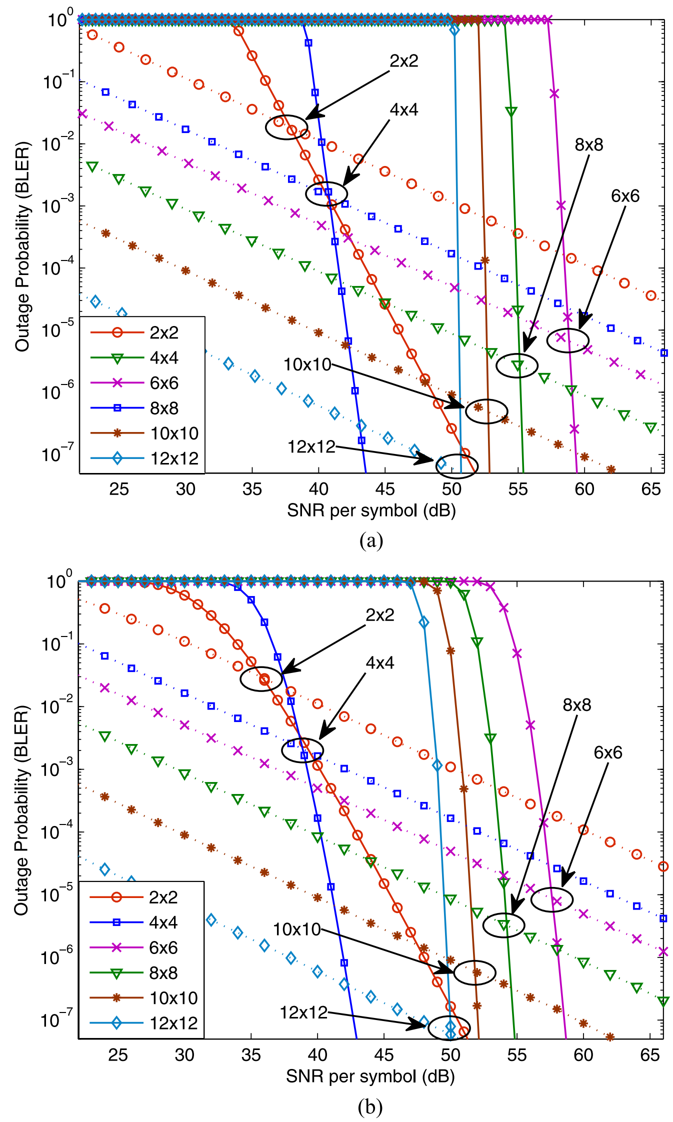

Fig. 5. Exact and high-SNR approximate outage probabilities for $R = 12$ bits/s/Hz in the spatially correlated Rayleigh fading channels with $\rho_t = \rho_r = 0.3$. Solid curves denote the outage probabilities of OSTBC, and dotted curves denote those of V-BLAST with an MMSE receiver. The crossover points of outage probabilities are marked with circles. (a) High-SNR approximate outage probabilities. (b) Exact outage probabilities.

To begin, we consider spatially correlated Rayleigh fading channels. The outage probabilities are evaluated, as an example, for spatial correlation coefficients of $\rho_t = \rho_r = 0.3$ and a spectral efficiency of $R = 12$ bits/s/Hz. The results are shown in Fig. 4, where the high-SNR approximate outage probabilities are derived from (3), (4), (12), and (13). Note that the analyses in Sections II and III are valid for any $k_r > 0$, subject to the constraint that $2^R/k_r > 1$ and $k_d > 0$ in the high-SNR approximate outage probabilities as given by (4) [18]. Let $P_{\text{out},V}(\gamma_s)$ and $P_{\text{out},O}(\gamma_s)$ denote the outage probabilities of V-BLAST with an MMSE receiver and OSTBC, respectively. In Fig. 4, we set the constant k_d in (4) to unity such that, at low SNR, we have $P_{\text{out},V}(\gamma_s) = P_{\text{out},O}(\gamma_s) = k_d = 1$, where the second equality follows from (3) and (4) and the last lines of (12) and (13) (i.e., $u = v = 0$ are substituted into (4)) [18]. Another constant, i.e., k_r, is chosen such that, at high SNR, the SNR gap between the high-SNR approximate outage probability and the exact one is small. In Fig. 4, the exact outage probabilities are obtained by numerically evaluating [30, Eqs. (6) and (9)] and [31, Eq. (20)] for V-BLAST with an MMSE receiver and OSTBC, respectively. Note that, in those equations, mutual information is normalized by the time duration of a space–time codeword (i.e., T as defined below (1)) for the computation of the outage probabilities. The curves in Fig. 4 are repeated in Fig. 5, which show that, when the number of transmit and receive antennas increases, as stated in the last paragraph in Section III, the crossover point of the outage probabilities in the correlated Rayleigh fading channels behaves as predicted by the analysis given by (23) (see Fig. 1).

As another example, Fig. 6 depicts the exact outage probabilities for spatial correlation coefficients of $\rho_t = \rho_r = 0.7$ and a spectral efficiency of $R = 12$ bits/s/Hz. It is shown that the

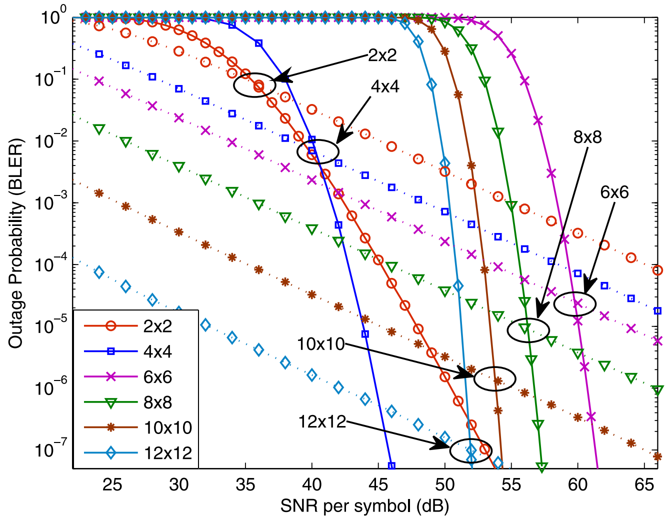

Fig. 6. Exact outage probabilities for $R = 12$ bits/s/Hz in the spatially correlated Rayleigh fading channels with $\rho_t = \rho_r = 0.7$. Solid curves denote the outage probabilities of OSTBC, and dotted curves denote those of V-BLAST with an MMSE receiver. The crossover points of outage probabilities are marked with circles.

crossover points in Fig. 6 exhibit the same behavior as those in Fig. 5. If we focus on an outage probability of 10^{-3}, in Fig. 6, OSTBC outperforms V-BLAST for $N_t = N_r = 2$ or 4, whereas the latter outperforms the former for $N_t = N_r = 6$, 8, 10, or 12. Note that this preference is a function of the target outage probability of the application. For example, if the target is 10^{-6}, OSTBC outperforms V-BLAST for $N_t = N_r = 2$, 4, 6, 8, or 10, and the latter outperforms the former only for $N_t = N_r = 12$. In addition, from Figs. 5 and 6, it is observed that the outage probability performance of V-BLAST tends to be more sensitive to the spatial correlation of MIMO channels than that of OSTBC. This is because, as stated in [32], spatial correlation leads to a disparity in the distribution of the spatial eigenmodes, which reduces the spatial multiplexing capability; spatial correlation in general leads to much less performance degradation for spatial diversity schemes than for spatial multiplexing [15], [19].

We next consider Rician fading channels. The outage probabilities are evaluated, as an example, for the Rician factor of $K = 2$ and a spectral efficiency of $R = 12$ bits/s/Hz. The numerical results are depicted in Fig. 7, where the high-SNR approximate and exact outage probabilities are derived in the same way as that for Fig. 4. The curves in Fig. 7 are repeated in Fig. 8, which indicate that the crossover points also exhibit the behavior as given by (23). Fig. 9 depicts the exact outage probabilities, as another example, for the Rician factor of $K = 5$ and a spectral efficiency of $R = 12$ bits/s/Hz. It is also shown that the crossover points in Fig. 9 behave as given by (23). Furthermore, in Figs. 8 and 9, it is shown that OSTBC works better in a channel with a stronger LOS, whereas V-BLAST fails to work well in the LOS case [15], [16].

The outage probabilities in i.i.d. Rayleigh fading channels for a spectral efficiency of $R = 4$ bits/s/Hz are shown in Figs. 10 and 11. It is again observed that the crossover points behave as given by (23). Fig. 12 depicts the outage probabilities for the number of antennas taken to be larger than those in

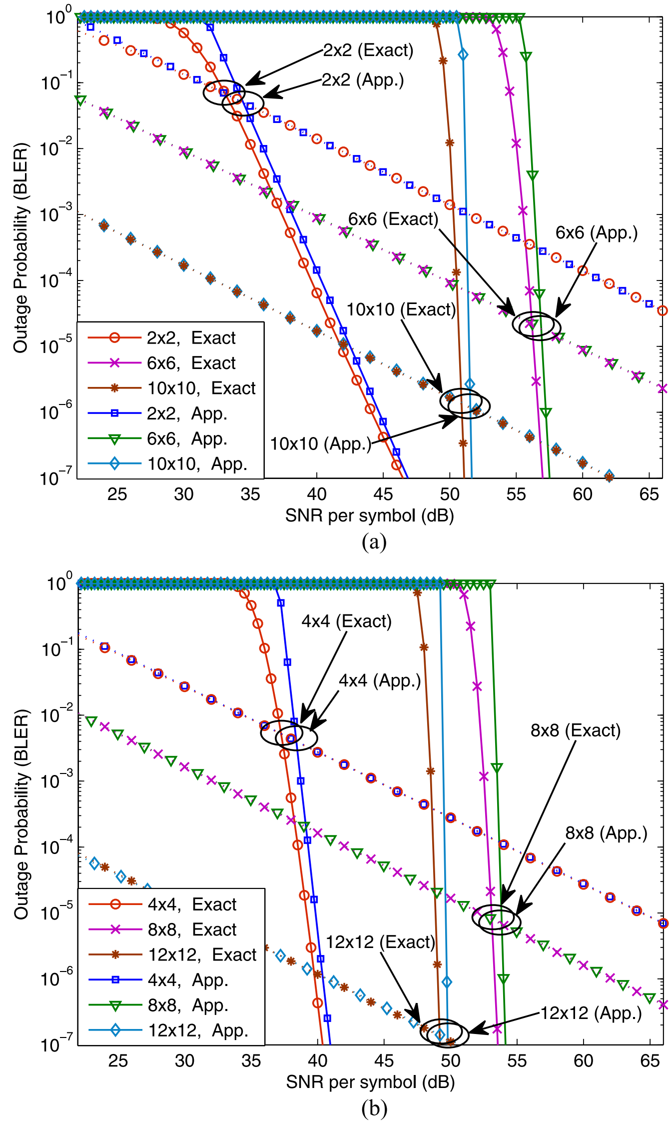

Fig. 7. Exact and high-SNR approximate outage probabilities for $R = 12$ bits/s/Hz in the Rician fading channels with $K = 2$. Solid curves denote the outage probabilities of OSTBC, and dotted curves denote those of V-BLAST with an MMSE receiver. The crossover points of outage probabilities are marked with circles. (a) 2×2, 6×6, and 10×10 MIMO systems. (b) 4×4, 8×8, and 12×12 MIMO systems.

Fig. 6, for spatial correlation coefficients of $\rho_t = \rho_r = 0.7$ and a spectral efficiency of $R = 12$ bits/s/Hz. It is shown that the crossover points also behave as predicted by (23).

Next, we evaluate the behavior of the crossover points for the case when the number of receive antennas increases, but the number of transmit antennas remains fixed. Figs. 13 and 14 depict the results of such a case for correlated Rayleigh fading channels having $\rho_t = \rho_r = 0.7$ and for the Rician fading channels with $K = 5$, when a spectral efficiency of $R = 12$ bits/s/Hz is used, respectively. When only the number of receive antennas increases, as described in the last paragraph in Section III, the crossover point of the outage probabilities in the correlated Rayleigh or Rician channels behaves as predicted by the analysis given by (29).

In Section IV, we presented the optimal space–time coding for the transmission of scalable sources. In the following,

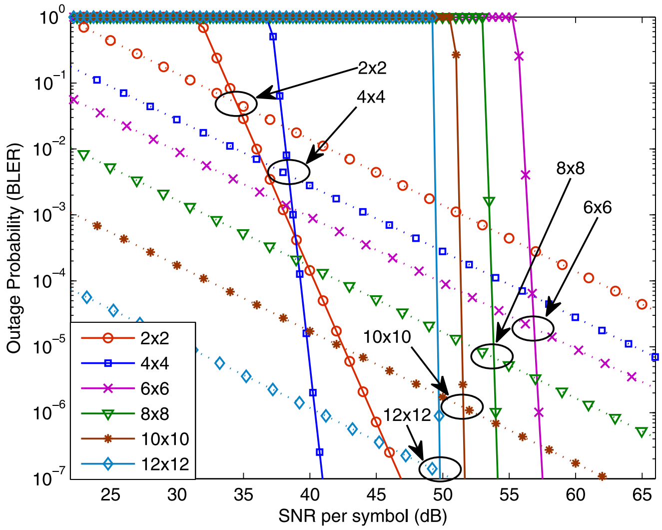

(a)

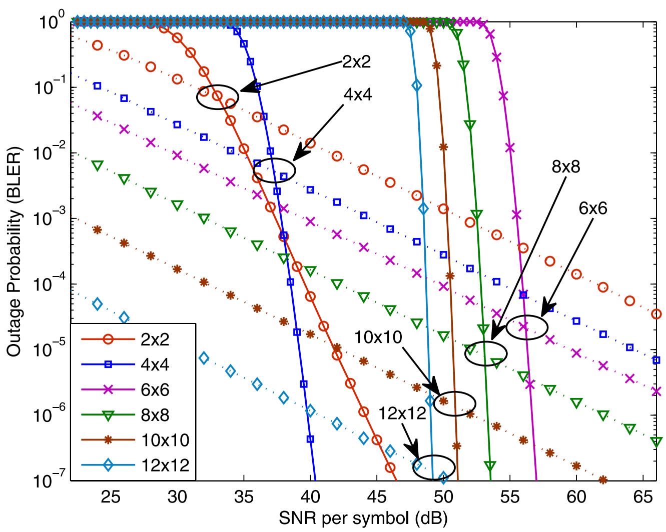

(b)

Fig. 8. Exact and high-SNR approximate outage probabilities for $R = 12$ bits/s/Hz in the Rician fading channels with $K = 2$. Solid curves denote the outage probabilities of OSTBC, and dotted curves denote those of V-BLAST with an MMSE receiver. The crossover points of outage probabilities are marked with circles. (a) High-SNR approximate outage probabilities. (b) Exact outage probabilities.

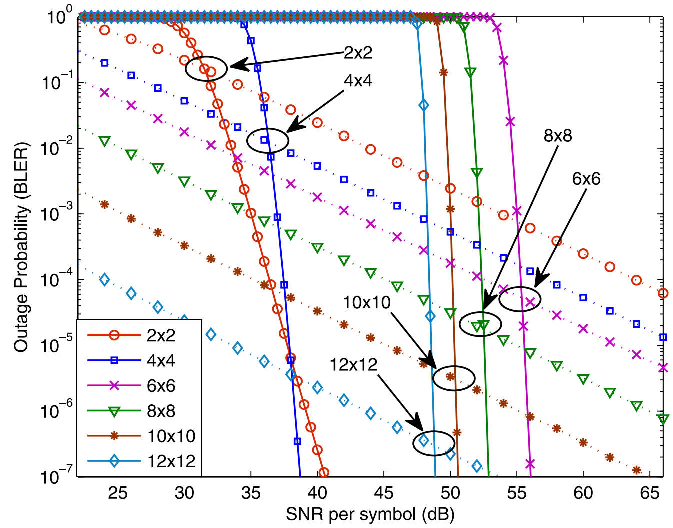

Fig. 9. Exact outage probabilities for $R = 12$ bits/s/Hz in the Rician fading channels with $K = 5$. Solid curves denote the outage probabilities of OSTBC, and dotted curves denote those of V-BLAST with an MMSE receiver. The crossover points of outage probabilities are marked with circles.

we will compare the performance of the optimal space–time coding and the suboptimal ones for scalable transmission. We evaluate the end-to-end performance measured by the expected distortion of the image for 8×8 MIMO systems using the source coder SPIHT [33] as an example and provide results for the standard 8 bpp 512×512 Lena image with a transmission rate of 0.5 bpp.

To begin, we summarize the evaluation of the expected distortion as stated in [18, Sec. V]. The system takes a compressed scalable bitstream from the source encoder and transforms it into a sequence of N_{pkt} packets with error detection and correction capability. Then, as shown in Fig. 2, the packets are encoded by the space–time codes. At the receiver, if a received packet is correctly decoded, the next packet is considered by the source decoder. Otherwise, the decoding is terminated, and the source is reconstructed from only the correctly decoded packets. We assume a slow-fading channel such that channel coefficients are nearly constant over an image, which consists of a sequence of N_{pkt} scalable packets, and the channel estimation at the receiver is perfect. Let $P_i(\dot{\gamma}_{s,i})$ denote the conditional probability of a decoding error of the ith packet $(1 \le i \le N_{\text{pkt}})$, conditioned on $\dot{\gamma}_{s,i}$, where $\dot{\gamma}_{s,i}$ is the instantaneous postprocessing SNR per symbol for the ith packet. Then, the probability that no decoding errors occur in the first n packets with an error in the next one, i.e., $P_{c,n}$, is given by

$$P_{c,n} = P_{n+1}(\dot{\gamma}_{s,n+1}) \prod_{i=1}^{n} \left(1 - P_i(\dot{\gamma}_{s,i})\right), \quad 1 \le n \le N_{\text{pkt}} - 1. \tag{30}$$

$P_{c,0} = P_1(\dot{\gamma}_{s,1})$ is the conditional probability of an error in the first packet, and $P_{c,N_{\text{pkt}}} = \prod_{i=1}^{N_{\text{pkt}}} (1 - P_i(\dot{\gamma}_{s,i}))$ is the conditional probability that all N_{pkt} packets are correctly decoded. Let d_n denote the distortion of the source using the first n packets for the source decoder $(0 \le n \le N_{\text{pkt}})$. Then, d_n can be expressed as $d_n = D(\sum_{i=1}^{n} r_i)$, where r_i is the number of source bits in the ith packet, $D(x)$ denotes the operational distortion-rate function of the source, and $d_0 = D(0)$ refers to the distortion when the decoder reconstructs the source without any of the received information. The expected distortion of the source, i.e., $E[D]$, can be expressed as (31), shown at the bottom of the next page, where $p(\dot{\gamma}_{s,i})$ is the probability density function of the instantaneous postprocessing SNR for the ith packet, i.e., $\dot{\gamma}_{s,i}$. Note that $p(\dot{\gamma}_{s,i})$ is a function of the average SNR per symbol γ_s, which is defined below (2), as well as the transmission data rate, power, and space–time code assigned to the ith packet. Thus, $E[D]$ is also a function of those system parameters.

Let D_i, P_i, and C_i denote the transmission data rate, power, and space–time code assigned to the ith packet, respectively. For given sets of $\{D_1, \ldots, D_{N_{\text{pkt}}}\}$ and $\{P_1, \ldots, P_{N_{\text{pkt}}}\}$ assigned to a sequence of N_{pkt} packets, one can find the optimal set of space–time codes $\mathbf{C}_{\text{opt}} = [C_1, \ldots, C_{N_{\text{pkt}}}]_{\text{opt}}$, which

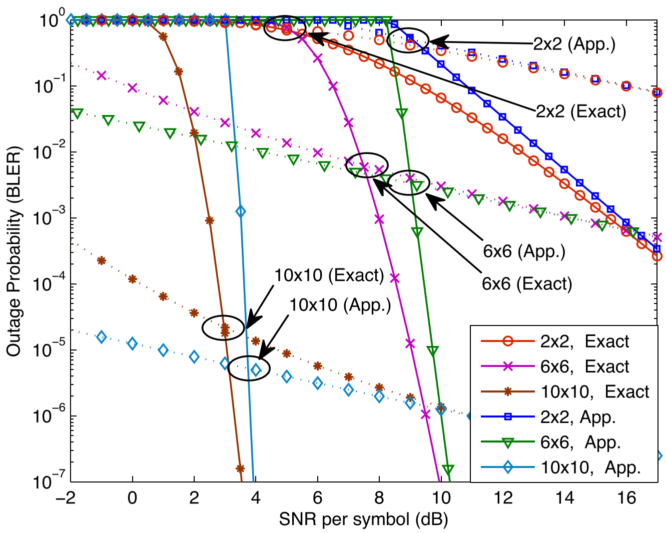

(a)

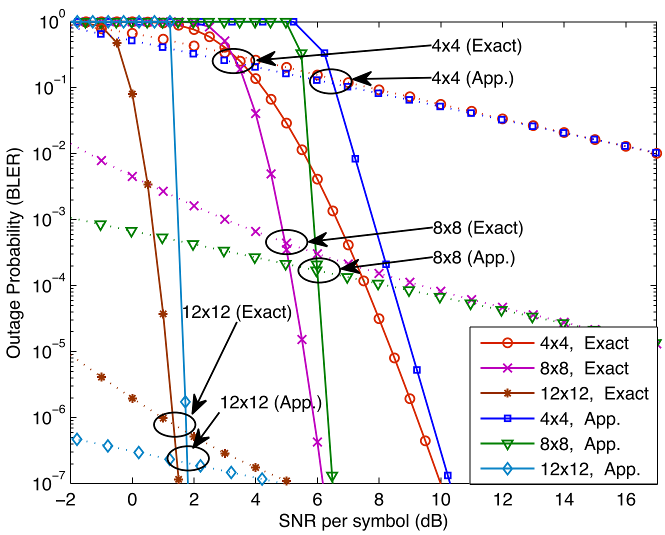

(b)

Fig. 10. Exact and high-SNR approximate outage probabilities for $R = 4$ bits/s/Hz in i.i.d. Rayleigh fading channels. Solid curves denote the outage probabilities of OSTBC, and dotted curves denote those of V-BLAST with an MMSE receiver. The crossover points of outage probabilities are marked with circles. (a) 2×2, 6×6, and 10×10 MIMO systems. (b) 4×4, 8×8, and 12×12 MIMO systems.

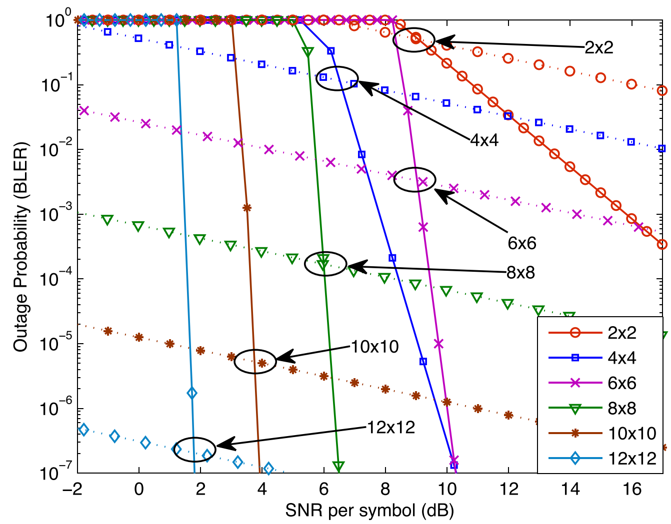

(a)

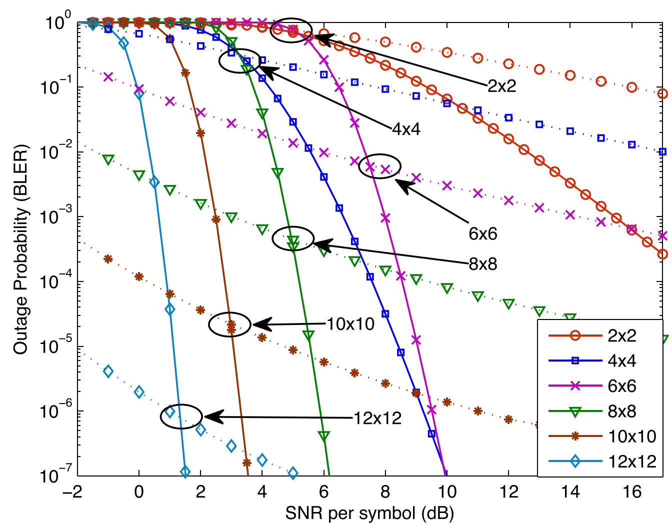

(b)

Fig. 11. Exact and high-SNR approximate outage probabilities for $R = 4$ bits/s/Hz in i.i.d. Rayleigh fading channels. Solid curves denote the outage probabilities of OSTBC, and dotted curves denote those of V-BLAST with an MMSE receiver. The crossover points of outage probabilities are marked with circles. (a) High-SNR approximate outage probabilities. (b) Exact outage probabilities.

minimizes the expected distortion over a range of average SNRs using the weighted cost function as follows:

$$\underset{C_1,\ldots,C_{N_{\mathrm{pkt}}}}{\arg\min} \frac{\int_0^\infty w(\gamma_s)E[D]d\gamma_s}{\int_0^\infty w(\gamma_s)d\gamma_s}, \tag{32}$$

where $w(\gamma_s)$ in [0, 1] is the weight function. For example, $w(\gamma_s)$ can be chosen such that

$$w(\gamma_s) = \begin{cases} 1, & \text{for } \gamma_{s,1} \leq \gamma_s \leq \gamma_{s,2}, \\ 0, & \text{otherwise.} \end{cases} \tag{33}$$

$$E[D] = \int_0^\infty \cdots \int_0^\infty \Bigg\{ D(0)P_1(\dot{\gamma}_{s,1}) + \sum_{n=1}^{N_{\mathrm{pkt}}-1} \left(D\left(\sum_{i=1}^{n} r_i\right) P_{n+1}(\dot{\gamma}_{s,n+1}) \prod_{i=1}^{n} (1 - P_i(\dot{\gamma}_{s,i})) \right)$$
$$+ D\left(\sum_{i=1}^{N_{\mathrm{pkt}}} r_i\right) \prod_{i=1}^{N_{\mathrm{pkt}}} (1 - P_i(\dot{\gamma}_{s,i})) \Bigg\} p(\dot{\gamma}_{s,1}), \ldots, p(\dot{\gamma}_{s,N_{\mathrm{pkt}}}) d\dot{\gamma}_{s,1}, \ldots, d\dot{\gamma}_{s,N_{\mathrm{pkt}}}. \tag{31}$$

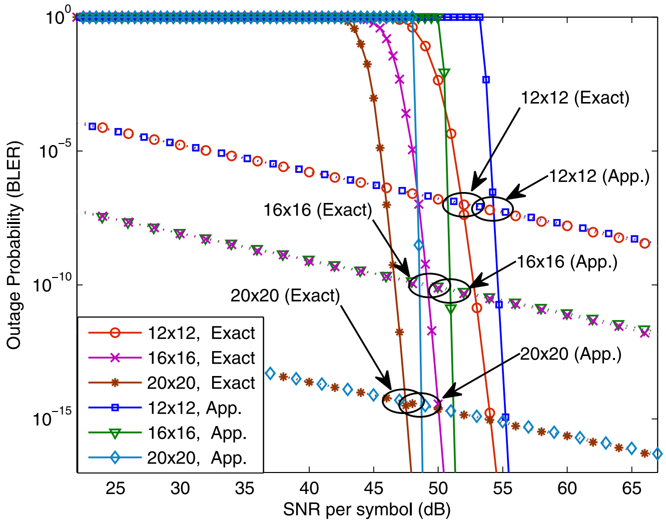

Fig. 12. Exact and high-SNR approximate outage probabilities for $R = 12$ bits/s/Hz in the spatially correlated Rayleigh fading channels with $\rho_t = \rho_r = 0.7$. Solid curves denote the outage probabilities of OSTBC, and dotted curves denote those of V-BLAST with an MMSE receiver. The crossover points of outage probabilities are marked with circles.

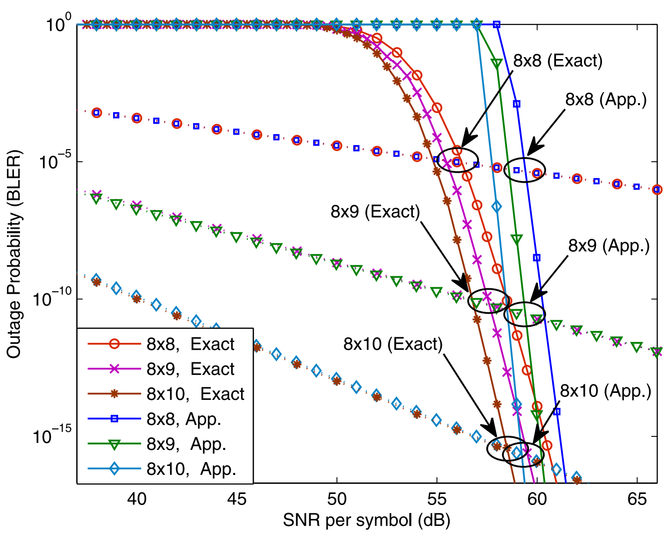

Fig. 13. Exact and high-SNR approximate outage probabilities for $R = 12$ bits/s/Hz in the spatially correlated Rayleigh fading channels with $\rho_t = \rho_r = 0.7$. Solid curves denote the outage probabilities of OSTBC, and dotted curves denote those of V-BLAST with an MMSE receiver. The crossover points of outage probabilities are marked with circles.

In broadcast systems, the weight function in (33) indicates that SNRs of multiple receivers are uniformly distributed in the range of $\gamma_{s,1} \leq \gamma_s \leq \gamma_{s,2}$. Eq. (32) indicates that the $\{C_1, \ldots, C_{N_{\text{pkt}}}\}$ are chosen such that the total sum of the expected distortion of the receivers distributed in the range of $\gamma_{s,1} \leq \gamma_s \leq \gamma_{s,2}$ is minimized. Note that the amount of computation involved in (32) exponentially grows as N_{pkt} increases. Alternatively, as presented in Section IV, we may choose the set of codes $\{C_1, \ldots, C_{N_{\text{pkt}}}\}$, with the constraint that V-BLAST should be assigned to the kth packet (i.e., OSTBC is excluded) if the packet has been encoded with V-BLAST in a pilot system as a result of the optimization.

To compare the image quality, we use the PSNR, which is defined as $10\log_{10}(255^2/E[D])$ (dB). The PSNR performance

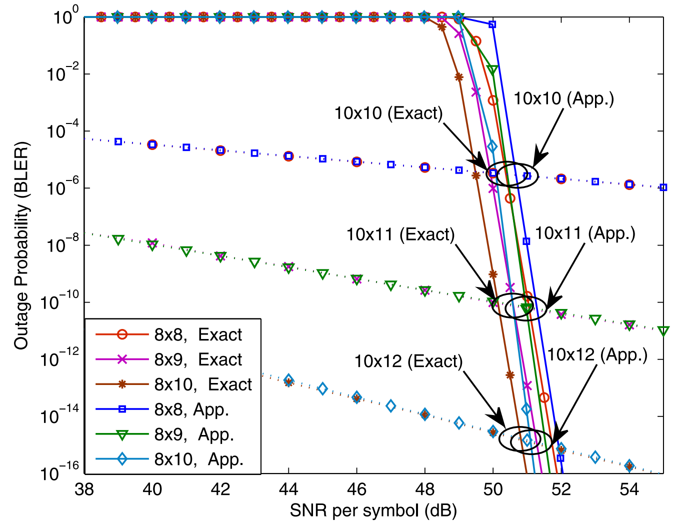

Fig. 14. Exact outage probabilities for $R = 12$ bits/s/Hz in the Rician fading channels with $K = 5$. Solid curves denote the outage probabilities of OSTBC, and dotted curves denote those of V-BLAST with an MMSE receiver. The crossover points of outage probabilities are marked with circles.

is evaluated as follows: We compute (32) using the expected distortion $E[D]$, given by (31), and the weight function $w(\gamma_s)$, given by (33). Next, with the optimal set of codes $\mathbf{C}_{\text{opt}} = [C_1, \ldots, C_{N_{\text{pkt}}}]_{\text{opt}}$ obtained from (32), we evaluate the PSNR over a range of SNRs given by (33).

The performance is evaluated, as an example, when a sequence of 12 scalable packets is transmitted (i.e., $N_{\text{pkt}} = 12$) in 8×8 MIMO systems, and we assume that the transmission data rates and powers are assigned to scalable packets in a manner that $\mathbf{R} = [12\ 10\ 8\ 7\ 6\ 5\ 4.5\ 4\ 3.5\ 3\ 2.5\ 2]$ (bits/s/Hz) and $\mathbf{P} = [0\ -1\ -2\ -3\ -4\ -5\ -6\ -7\ -8\ -9\ -10\ -11]$ (dB), where the ith component of $\mathbf{R}$ is the spectral efficiency employed by the ith packet, and the ith component of $\mathbf{P}$ is the ratio of the transmission power of the ith packet to that of the first packet. With this specific setup, the optimal set of space–time codes, which is computed from (32), is given by $C_1 = \cdots = C_4 =$ V-BLAST, $C_5 = C_6 =$ OSTBC, $C_7 = C_8 = C_9 =$ V-BLAST, and $C_{10} = C_{11} = C_{12} =$ OSTBC in the correlated Rayleigh fading channel of $\rho_t = \rho_r = 0.7$.

Fig. 15 shows the PSNR of such an optimal set of space–time codes, in addition to showing the PSNRs of other suboptimal sets of codes, such as the sets at the 75th and 50th percentiles among the sets of codes,[3] and the worst set of codes, which has the poorest performance. Fig. 15 also shows the PSNR corresponding to the expected distortion that is averaged over all the possible sets of space–time codes. From this example, it is seen that the PSNR performance of the scalable source is sensitive to the way space–time codes are assigned to a sequence of N_{pkt} packets, in part due to their unequal target error rates in the bitstream. Fig. 15 also depicts the PSNR performance when (32) is computed with the constraint presented in Section IV. A 2×2 MIMO system has been employed as a pilot system. With the same setup used for an 8×8 target system, the optimal set of codes in a 2×2 pilot system,

[3]The number of possible sets of space–time codes is $2^{N_{\text{pkt}}} = 4096$ in this case.

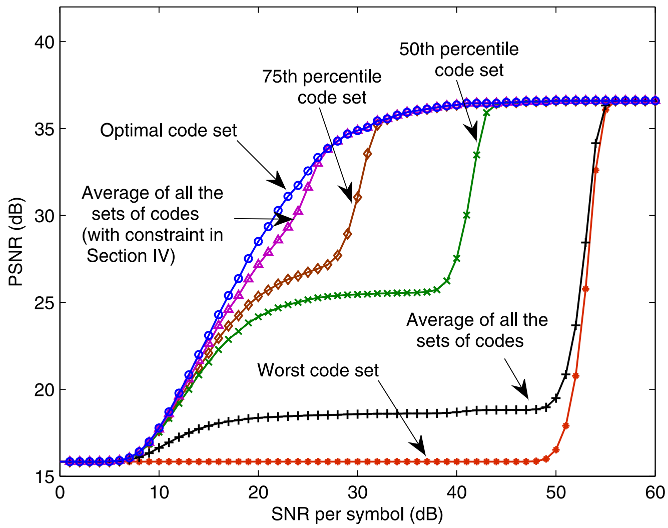

Fig. 15. PSNR performances of the optimal set of space–time codes and suboptimal ones for the transmission of the embedded 512 × 512 Lena image for 8 × 8 MIMO systems in spatially correlated Rayleigh fading channels with $\rho_t = \rho_r = 0.7$.

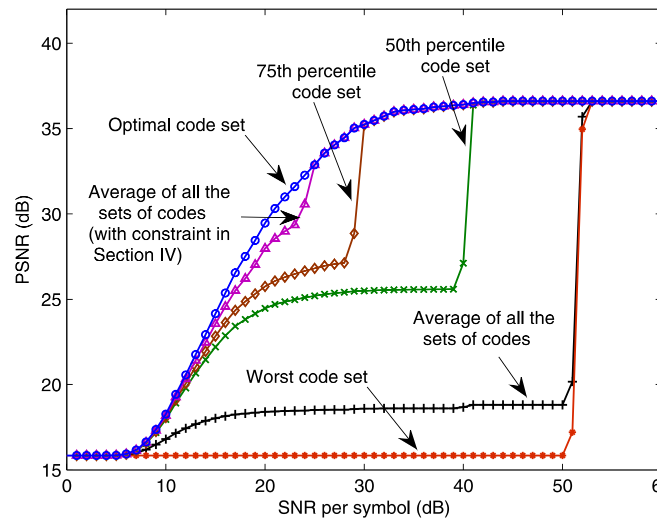

Fig. 16. PSNR performances of the optimal set of space–time codes and suboptimal ones for the transmission of the embedded 512 × 512 Lena image for 8 × 8 MIMO systems in Rician fading channels with $K = 5$.

which is computed from (32), is given by $C_1 = C_2 = C_3 =$ V-BLAST, $C_4 = C_5 = C_6 =$ OSTBC, $C_7 = C_8 =$ V-BLAST, and $C_9 = \cdots = C_{12} =$ OSTBC (i.e., $N_{\rm vb} = 5$). Recall that, with the constraint in Section IV, the number of possible sets of space–time codes in a target system is reduced from $2^{N_{\rm pkt}}$ to $2^{N_{\rm pkt} - N_{\rm vb}}$ (i.e., from 4096 to 128 in this example).

We note that the same optimal set of space–time codes has been obtained when (32) is computed with and without the constraint. That is, without losing any PSNR performance, the computational complexity involved with the optimization can be reduced by exploiting the monotonic behavior of the crossover point, as shown in Fig. 1. It is further seen that the PSNR, which corresponds to the expected distortion averaged over all the possible sets of codes, becomes much better when the constraint in Section IV is introduced, which shows that, on average, the constraint is a good strategy for the space–time coding of scalable sources.

Fig. 16 shows the PSNR performances in the Rician fading channel of $K = 5$, where we use the same system parameters as those for the correlated Rayleigh channel whose results are shown in Fig. 15. We also note that, in Fig. 16, the same optimal set of space–time codes has been obtained when (32) is computed with and without the constraint. Furthermore, like the case in Fig. 15, the PSNR corresponding to the expected distortion averaged over all the possible sets of space–time codes becomes better when the constraint in Section IV is used. This indicates that the constraint is also a good optimization strategy in Rician fading channels.

We note that, in addition to embedded images, our analysis in Sections III and IV can be also applied to scalable video. In scalable video, the base layer is more important than the enhancement layer. If we split the base layer into multiple packets, those packets often have a similar level of importance. However, the enhancement layer, for example, with medium-grain scalability, can usually be split into multiple packets with successively decreasing importance. Hence, for real-time scalable video, we can apply our analytical results to the sequence of high-importance base layer packets and successively less important enhancement layer packets.

Finally, we note that, when selecting the optimal space–time code in an 8 × 8 MIMO system, in addition to the OSTBC that uses all the eight transmit antennas with the spatial multiplexing rate of $r_s = 1/2$, we also consider the OSTBC that uses only two or four transmit antennas with $r_s = 1$ or 3/4, respectively. That is, for an 8 × 8 MIMO system, the OSTBC scheme that uses either a 2 × 8 or a 4 × 8 antenna configuration is also considered. The motivation for considering such an OSTBC scheme is as follows: The OSTBCs can be classified into three groups, according to their maximum achievable spatial multiplexing rates: 1) $r_s = 1/2$ for $N_t \geq 5$; 2) $r_s = 3/4$ for $N_t = 3$ or 4; and 3) $r_s = 1$ for $N_t = 2$. In Appendix B, we show that, for two OSTBCs, which belong to distinct groups earlier, there exists a crossover point of their outage probabilities; furthermore, the crossover point in outage probability is a strictly decreasing function in spectral efficiency. This indicates that, as an example, for a $3 \times N_r$ MIMO system, it is possible that the OSTBC that uses only two transmit antennas with $r_s = 1$ (i.e., OSTBC that uses a $2 \times N_r$ configuration) outperforms the OSTBC that uses all the three transmit antennas with $r_s = 3/4$ (i.e., OSTBC using a $3 \times N_r$ configuration). Note that which OSTBC scheme performs better depends on the target error rate of the application and the spectral efficiency employed by the system. For this reason, in 8 × 8 MIMO systems, we consider the OSTBC scheme that uses only two or four transmit antennas and the one that uses all the eight transmit antennas as a candidate space–time code.

VI. Conclusion

Because of increasing use of higher carrier frequencies and the advances in the computational capability of hardware, a MIMO system is capable of employing a large number of antennas. When a series of scalable sources is transmitted over MIMO channels, space–time coding should be optimized for each individual rate–distortion characteristic. For a large number of antennas, however, the optimization is complex. To address this matter, we suggested an efficient method to optimize the space–time coding of scalable sources.

To begin, we analyzed the crossover point of the outage probabilities of V-BLAST, using either a linear or an ML receiver, with OSTBC, in terms of the number of antennas. The results showed that, as the number of antennas increases, the crossover point in outage probability monotonically decreases, which were proven for arbitrary spectral efficiency employed by the system. These results are conceptually depicted in Fig. 1, and we are unaware of any other literature that either states or proves them. The results are valid in spatially correlated Rayleigh or Rician fading channels, as well as in i.i.d. Rayleigh fading channels.

Based on the analysis, we suggested a method to optimally assign V-BLAST or OSTBC to a sequence of scalable packets over spatially correlated Rayleigh or Rician channels with a large number of antennas. It was shown that, without any PSNR degradation, the computational complexity involved with optimal space–time coding is exponentially reduced by the use of the suggested method. Furthermore, the PSNR performance averaged over all the possible sets of space–time codes becomes better when our method is used, which indicates that, on the average, it is a good strategy for the space–time coding of multimedia scalable sources. The technical approach in this paper, which was used to analyze the tradeoff between space–time codes in terms of their target error rates and the number of antennas, may be used for other space–time codes such as quasi-OSTBC or Golden codes as future work.

Appendix A
Crossover Point for V-BLAST With a Maximum Likelihood Receiver and Orthogonal Space Time Block Codes

The DMT characteristic of V-BLAST with an ML receiver, i.e., $d_{V,\mathrm{ML}}(r)$, is given by [22]

$$d_{V,\mathrm{ML}}(r) = \begin{cases} N_r - N_r r/N_t, & \text{for } 0 \le r \le N_t, \\ 0, & \text{for } N_t \le r < \infty. \end{cases} \tag{34}$$

Using (13) and (34), we set $d_1(r) = d_{V,\mathrm{ML}}(r)$ and $d_2(r) = d_O(r)$ in (5). Then, from (13), (34), and $N_t > r_s$, it follows that, for the range of $0 < r \le r_s$, the condition of (6) is satisfied. Moreover, from $N_r \ge N_t \ge 2$, we have

$$d_{V,\mathrm{ML}}(0) - d_O(0) = N_r(1 - N_t) < 0, \tag{35}$$
$$d_{V,\mathrm{ML}}(r_s) - d_O(r_s) = N_r(1 - r_s/N_t) > 0. \tag{36}$$

Eqs. (35) and (36) meet the conditions of (7) and (8), respectively, when we set $\alpha = \varepsilon$ and $\beta = r_s$, where $\varepsilon > 0$ is an arbitrarily small positive number. Hence, (11) holds, and this tells us that there exists a crossover point of the outage probabilities for V-BLAST with an ML receiver and OSTBC in the range of $(2^R/k_r)^{1/r_s} \le \gamma_s < \infty$. In addition, from (10), (13), and (34), P^*_{out} is given by

$$P^*_{\mathrm{out}} = k_d \left(\frac{2^R}{k_r}\right)^{\frac{(1-N_t/r_s)N_r}{N_t-1}}. \tag{37}$$

Letting $N_t = N_r = n$ in (37), we have

$$P^*_{\mathrm{out}} = k_d \left(\frac{2^R}{k_r}\right)^{\frac{n-n^2/r_s}{n-1}}. \tag{38}$$

Let $s(n) = (n - n^2/r_s)/(n-1)$ be the exponent of P^*_{out} given by (38). If we assume that n is a real number, $ds(n)/dn$ can be expressed as

$$\frac{ds(n)}{dn} = \frac{-n^2 + 2n - r_s}{r_s(n-1)^2}. \tag{39}$$

Let $w(n) = -n^2 + 2n - r_s$ be the numerator of $ds(n)/dn$. It can be shown that $w(n)$ is a strictly decreasing function in n for $n \ge 2$. From this and $n\ (= N_t = N_r) \ge 2$, $w(n)$ satisfies

$$w(n) \le w(2) = -r_s < 0. \tag{40}$$

Eqs. (39) and (40) show that

$$\frac{ds(n)}{dn} < 0, \quad \text{for } n \ge 2. \tag{41}$$

From (38), (41), and $k_d > 0$ and $2^R/k_r > 1$ given in Section II, it is seen that P^*_{out} is a strictly decreasing function in $n\ (\ge 2)$, regardless of a given spectral efficiency R. In other words, for any fixed spectral efficiency, as the number of antennas, i.e., $N_r = N_t\ (\ge 2)$, increases, the crossover point in the outage probability monotonically decreases. Thus, the same argument given by (23) can be also made for V-BLAST with an ML receiver and OSTBC.

In addition, from $N_t \ge 2$ and $1/2 \le r_s \le 1$, it follows that P^*_{out}, given by (37), is a strictly decreasing function in $N_r\ (\ge N_t \ge 2)$, regardless of a given spectral efficiency R, as well as a given number of transmit antennas N_t. That is, for any fixed spectral efficiency and any fixed number of transmit antennas, as only the number of receive antennas increases, the crossover point in the outage probability monotonically decreases. Hence, the results given by (29) also hold for V-BLAST with an ML receiver and OSTBC.

Appendix B
Crossover Point for Orthogonal Space Time Block Codes With Distinct Spatial Multiplexing Rates

Let $d^x_O(r)$, $d^y_O(r)$, and $d^z_O(r)$ denote the DMT characteristics of the OSTBCs with spatial multiplexing rates r_s = 1/2, 3/4, and 1, respectively. Then, from (13), we have

$$d^x_O(r) = \begin{cases} N_r N^x_t - 2N_r N^x_t\, r, & \text{for } 0 \le r \le \frac{1}{2}, \\ 0, & \text{for } \frac{1}{2} \le r < \infty, \end{cases} \tag{42}$$

$$d^y_O(r) = \begin{cases} N_r N^y_t - \frac{4}{3} N_r N^y_t\, r, & \text{for } 0 \le r \le \frac{3}{4}, \\ 0, & \text{for } \frac{3}{4} \le r < \infty, \end{cases} \tag{43}$$

$$d^z_O(r) = \begin{cases} 2N_r - 2N_r\, r, & \text{for } 0 \le r \le 1, \\ 0, & \text{for } 1 \le r < \infty, \end{cases} \tag{44}$$

where $N^x_t \ge 5$, and $N^y_t = 3$ or 4. In the following, we analyze the crossover point of the outage probabilities of the OSTBCs, which have different spatial multiplexing rates.

1) *The OSTBCs with $r_s = 1/2$ and $r_s = 3/4$*: From (42) and (43), it follows that, for the range of $0 < r \leq 1/2$, the condition of (6) is met if we set $d_1(r) = d_O^y(r)$ and $d_2(r) = d_O^x(r)$ in (5). In addition, from $N_t^x \geq 5$ and $N_t^y = 3$ or 4, it can be shown that

$$d_O^y(0) - d_O^x(0) = N_r(N_t^y - N_t^x) < 0, \quad (45)$$
$$d_O^y\left(\frac{1}{2}\right) - d_O^x\left(\frac{1}{2}\right) = \frac{1}{3}N_r N_t^y > 0. \quad (46)$$

Eqs. (45) and (46) meet the conditions of (7) and (8), respectively, when we set $\alpha = \varepsilon$ and $\beta = 1/2$, where $\varepsilon > 0$ is an arbitrarily small positive number. Hence, from (11), we have

$$P_{\text{out},O}^y(\gamma_s) < P_{\text{out},O}^x(\gamma_s), \quad \text{for } \left(\frac{2^R}{k_r}\right)^2 < \gamma_s < \gamma_s^*,$$
$$P_{\text{out},O}^y(\gamma_s) > P_{\text{out},O}^x(\gamma_s), \quad \text{for } \gamma_s^* < \gamma_s < \infty, \quad (47)$$

where $P_{\text{out},O}^x(\gamma_s)$ and $P_{\text{out},O}^y(\gamma_s)$ denote the outage probabilities of the OSTBCs with $r_s = 1/2$ and 3/4, respectively. That is, there exists a crossover point of the outage probabilities of the OSTBCs with $r_s = 1/2$ and 3/4, and this holds for any number of receive antennas N_r and any spectral efficiency R. In addition, from (10), (42), and (43), it can be shown that the crossover point of the outage probabilities is given by $P_{\text{out}}^* = k_d(2^R/k_r)^{-2N_r N_t^x N_t^y / 3(N_t^x - N_t^y)}$. For $N_t^x \geq 5$ and $N_t^y = 3$ or 4, we have $N_r N_t^x N_t^y / (N_t^x - N_t^y) > 0$. From this and $k_d > 0$ and $2^R/k_r > 1$ given in Section II, it is seen that P_{out}^* is a strictly decreasing function in R.

2) *The OSTBCs with $r_s = 1/2$ and $r_s = 1$*: From (42) and (44), it is seen that, for the range of multiplexing gain, i.e., $0 < r \leq 1/2$, the condition of (6) is satisfied if we set $d_1(r) = d_O^z(r)$ and $d_2(r) = d_O^x(r)$ in (5). In addition, from $N_t^z \geq 5$, it can be shown that

$$d_O^z(0) - d_O^x(0) = N_r(2 - N_t^z) < 0, \quad (48)$$
$$d_O^z\left(\frac{1}{2}\right) - d_O^x\left(\frac{1}{2}\right) = N_r > 0. \quad (49)$$

Eqs. (48) and (49) satisfy the conditions of (7) and (8), respectively, when setting $\alpha = \varepsilon$ and $\beta = 1/2$, where $\varepsilon > 0$ denotes an arbitrarily small positive number. Thus, from (11), we have

$$P_{\text{out},O}^z(\gamma_s) < P_{\text{out},O}^x(\gamma_s), \quad \text{for } \left(\frac{2^R}{k_r}\right)^2 < \gamma_s < \gamma_s^*,$$
$$P_{\text{out},O}^z(\gamma_s) > P_{\text{out},O}^x(\gamma_s), \quad \text{for } \gamma_s^* < \gamma_s < \infty, \quad (50)$$

where $P_{\text{out},O}^z(\gamma_s)$ is the outage probability of the OSTBC with $r_s = 1$. This indicates that there exists a crossover point of the outage probabilities of the OSTBCs with $r_s = 1/2$ and 1, which is valid for any number of receive antennas N_r and any spectral efficiency R. Furthermore, from (10), (42), and (44), it can be shown that the crossover point of the outage probabilities is given by $P_{\text{out}}^* = k_d(2^R/k_r)^{-2N_t^x N_r/(N_t^x - 2)}$. Since $N_t^x N_r/(N_t^x - 2) > 0$ for $N_t^x \geq 5$ and from $2^R/k_r > 1$ given in Section II, it follows that P_{out}^* is a strictly decreasing function in R.

3) *OSTBCs with $r_s = 3/4$ and $r_s = 1$*: In a similar manner, it can be shown that

$$P_{\text{out},O}^z(\gamma_s) < P_{\text{out},O}^y(\gamma_s), \quad \text{for } \left(\frac{2^R}{k_r}\right)^{\frac{4}{3}} < \gamma_s < \gamma_s^*,$$
$$P_{\text{out},O}^z(\gamma_s) > P_{\text{out},O}^y(\gamma_s), \quad \text{for } \gamma_s^* < \gamma_s < \infty. \quad (51)$$

In addition, the crossover point of the outage probabilities $P_{\text{out}}^* = k_d(2^R/k_r)^{-2N_t^y N_r/3(N_t^y - 2)}$ is a strictly decreasing function in R.

References

[1] Z. Yang and X. Wang, "Scalable video broadcast over downlink MIMO-OFDM systems," *IEEE Trans. Circuits Syst. Video Technol.*, vol. 23, no. 2, pp. 212–223, Feb. 2013.

[2] H. Zhang, Y. Zheng, M. A. Khojastepour, and S. Rangarajan, "Cross-layer optimization for streaming scalable video over fading wireless networks," *IEEE J. Sel. Areas Commun.*, vol. 28, no. 3, pp. 344–353, Apr. 2010.

[3] S.-H. Chang, P. C. Cosman, and L. B. Milstein, "Channel coding for progressive images in a 2-D time–frequency OFDM block with channel estimation errors," *IEEE Trans. Image Process.*, vol. 20, pp. 1061–1076, Apr. 2011.

[4] H. Schwarz, D. Marpe, and T. Wiegand, "Overview of the scalable video coding extension of H.264/AVC," *IEEE Trans. Circuits Syst. Video Technol.*, vol. 17, no. 9, pp. 1103–1120, Sep. 2007.

[5] J. Reichel, H. Schwarz, and M. Wien, "Scalable video coding–Working draft 1," *Joint Video Team of ITU-T VCEG and ISO/IEC MPEG, Doc. JVT-N*, vol. 20, p. 2005, Jul. 2005.

[6] Y. Jin and H.-J. Lee, "A block-based pass-parallel SPIHT algorithm," *IEEE Trans. Circuits Syst. Video Technol.*, vol. 22, no. 7, pp. 1064–1075, Jul. 2012.

[7] D. Taubman and M. Marcellin, *JPEG2000: Image Compression Fundamentals, Standards, and Practice*. Norwell, MA, USA: Kluwer, 2001.

[8] S. M. Alamouti, "A simple transmit diversity technique for wireless communications," *IEEE J. Sel. Areas Commun.*, vol. 16, no. 8, pp. 1451–1458, Oct. 1998.

[9] V. Tarokh, H. Jafarkhani, and A. R. Calderbank, "Space–time block codes from orthogonal designs," *IEEE Trans. Inf. Theory*, vol. 45, no. 5, pp. 1456–1467, Jul. 1999.

[10] G. J. Foschini, "Layered space–time architecture for wireless communication in a fading environment when using multiple antennas," *Bell Labs. Tech. J.*, vol. 1, no. 2, pp. 41–59, Autumn 1996.

[11] R. Louie, M. McKay, and I. Collings, "Open-loop spatial multiplexing and diversity communications in ad hoc networks," *IEEE Trans. Inf. Theory*, vol. 57, no. 1, pp. 317–344, Jan. 2011.

[12] T. Rappaport *et al.*, "Millimeter wave mobile communications for 5G cellular: It will work!" *IEEE Access*, vol. 1, pp. 335–349, May 2013.

[13] D. Tse and P. Viswanath, *Fundamentals of Wireless Communication*. New York, NY, USA: Cambridge Univ. Press, 2005.

[14] H. Shin and J. H. Lee, "Capacity of multiple-antenna fading channels: Spatial fading correlation, double scattering, and keyhole," *IEEE Trans. Info. Theory*, vol. 49, no. 10, pp. 2636–2647, Oct. 2003.

[15] R. Mesleh, H. Haas, S. Sinanovic, C. W. Ahn, and S. Yun, "Spatial modulation," *IEEE Trans. Veh. Technol.*, vol. 57, no. 4, pp. 2228–2241, Jul. 2008.

[16] H. Yang, "A road to future broadband wireless access: MIMO-OFDM based air interface," *IEEE Commun. Mag.*, vol. 43, no. 1, pp. 53–60, Jan. 2005.

[17] L. Zheng and D. N. C. Tse, "Diversity and multiplexing: A fundamental tradeoff in multiple-antenna channels," *IEEE Trans. Inf. Theory*, vol. 49, no. 5, pp. 1073–1096, May 2003.

[18] S.-H. Chang, J. P. Choi, P. C. Cosman, and L. B. Milstein, "Optimization of multimedia progressive transmission over MIMO channels," *IEEE Trans. Veh. Technol.*, vol. 65, no. 3, pp. 1244–1260, Mar. 2016.

[19] A. Forenza, M. R. McKay, A. Pandharipande, R. W. Heath, Jr., and I. B. Collings, "Adaptive MIMO transmission for exploiting the capacity of spatially correlated channels," *IEEE Trans. Veh. Technol.*, vol. 56, no. 2, pp. 619–630, Mar. 2007.
[20] A. Forenza, M. R. McKay, I. B. Collings, and R. W. Heath, Jr., "Switching between OSTBC and spatial multiplexing with linear receivers in spatially correlated MIMO channels," in *Proc. IEEE 63rd VTC*, Melbourne, Vic., Australia, May 2006, pp. 1387–1391.
[21] G. Taricco and E. Riegler, "On the ergodic capacity of correlated Rician fading MIMO channels with interference," *IEEE Trans. Inf. Theory*, vol. 57, no. 7, pp. 4123–4137, Jul. 2011.
[22] C. Oestges and B. Clerckx, *MIMO Wireless Communications*. Orlando, FL, USA: Academic, 2007.
[23] O. Tirkkonen and A. Hottinen, "Square-matrix embeddable space–time block codes for complex signal constellations," *IEEE Trans. Inf. Theory*, vol. 48, no. 2, pp. 384–395, Feb. 2002.
[24] R. Narasimhan, "Finite-SNR diversity-multiplexing tradeoff for correlated Rayleigh and Rician MIMO channels," *IEEE Trans. Inf. Theory*, vol. 52, no. 9, pp. 3965–3979, Sep. 2006.
[25] L. Zhao, W. Mo, Y. Ma, and Z. Wang, "Diversity and multiplexing tradeoff in general fading channels," *IEEE Trans. Inf. Theory*, vol. 53, no. 4, pp. 1549–1557, Apr. 2007.
[26] L. Toni, Y. S. Chan, P. C. Cosman, and L. B. Milstein, "Channel coding for progressive images in a 2-D time–frequency OFDM block with channel estimation errors," *IEEE Trans. Image Process.*, vol. 18, no. 11, pp. 2476–2490, Nov. 2009.
[27] V. M. Stankovic, R. Hamzaoui, Y. Charfi, and Z. Xiong, "Real-time unequal error protection algorithms for progressive image transmission," *IEEE J. Sel. Areas Commun.*, vol. 21, no. 10, pp. 1526–1535, Dec. 2003.
[28] S.-H. Chang, P. C. Cosman, and L. B. Milstein, "Iterative channel decoding of FEC-based multiple description codes," *IEEE Trans. Image Process.*, vol. 21, no. 3, pp. 1138–1152, Mar. 2012.
[29] G. H. Golub and C. F. Van Loan, *Matrix Computations*, 3rd ed. Baltimore, MD, USA: The Johns Hopkins Univ. Press, 1996.
[30] K. Raj, G. Caire, and A. L. Moustakas, "Asymptotic performance of linear receivers in MIMO fading channels," *IEEE Trans. Inf. Theory*, vol. 55, no. 10, pp. 4398–4418, Oct. 2009.
[31] S.-H. Chang, P. C. Cosman, and L. B. Milstein, "Optimal transmission of progressive sources based on the error probability analysis of SM and OSTBC," *IEEE Trans. Veh. Technol.*, vol. 63, no. 1, pp. 94–106, Jan. 2014.
[32] A. Lozano and N. Jindal, "Transmit diversity vs. spatial multiplexing in modern MIMO systems," *IEEE Trans. Wireless Commun.*, vol. 9, no. 1, pp. 186–197, Jan. 2010.
[33] A. Said and W. A. Pearlman, "A new, fast, and efficient image codec based on set partitioning in hierarchical trees," *IEEE Trans. Circuits Syst. Video Technol.*, vol. 6, no. 3, pp. 243–250, Jun. 1996.

Seok-Ho Chang (S'07–M'10) received the B.S. and M.S. degrees in electrical engineering from Seoul National University, Seoul, South Korea, in 1997 and 1999, respectively, and the Ph.D. degree in electrical engineering from the University of California, San Diego, CA, USA, in 2010.

From 1999 to 2005, he was with LG Electronics, Anyang, South Korea, where he was involved in development of WCDMA (3GPP) base/mobile station modem chips. In 2006, he was with POSCO ICT, Sungnam, South Korea, where he worked on mobile WiMax systems. From 2010 to 2011, he was with the University of California, San Diego as a Postdoctoral Scholar, where he was engaged in the joint optimization of wireless multimedia systems. From 2011 to 2012, he was with Qualcomm Inc., San Diego, as a Staff Engineer, where he was involved in design and development of 4G cellular modem chips. Since September 2012, he has been an Associate Professor with the Department of Computer Science and Engineering, Dankook University, Yongin, South Korea. His research interests include wireless/wireline communication theory, multiuser multiple-input multiple-output (MIMO) systems, joint optimization of wireless systems, signal processing, and learning-based multimedia communications

Jihwan P. Choi (S'01–M'06) received the B.S. degree from Seoul National University, Seoul, South Korea, in 1998 and the S.M. and Ph.D. degrees in electrical engineering and computer science from Massachusetts Institute of Technology (MIT), Cambridge, MA, USA, in 2000 and 2006, respectively.

From 1999 to 2006, he participated in the Next Generation Internet satellite network project at MIT. From 2006 to 2012, he was a Principal System Engineer with the Wireless Research and Development Group, Marvell Semiconductor, Inc., Santa Clara, CA, USA, for mobile system design and standardization of third-/fourth-generation commercial wireless communications, including Worldwide Interoperability for Microwave Access (WiMAX) and Third-Generation Partnership Project Long-Term Evolution. He is currently an Assistant Professor with the Department of Information and Communication Engineering, Daegu Gyeongbuk Institute of Science and Technology, Daegu, South Korea. His research interests are in cross-layer system design for space/wireless networks.

Pamela C. Cosman (S'88–M'93–SM'00–F'08) received the B.S.(Hons.) degree in electrical engineering from California Institute of Technology, Pasadena, CA, USA, in 1987 and the Ph.D. degree in electrical engineering from Stanford University, Stanford, CA, in 1993.

She was a National Science Foundation Postdoctoral Fellow with Stanford University and a Visiting Professor with the University of Minnesota, Minneapolis, MN, USA, during 1993–1995. In 1995, she joined the faculty of the Department of Electrical and Computer Engineering, University of California at San Diego, La Jolla, CA, where she is currently a Professor and an Associate Dean for Students of the Jacobs School of Engineering. From 2006 to 2008, she was the Director of the Center for Wireless Communications with the University of California at San Diego. Her research interests are in the areas of image and video compression and processing and wireless communications.

Dr. Cosman has been a member of the Technical Program Committee or the Organizing Committee for numerous conferences, including the European Signal Processing Conference (EUSIPCO) in 1998; the Advanced Concepts for Intelligent Vision Systems during 2002–2012; the International Conference on Internet Surveillance and Protection in 2003; the Asilomar Conference on Signals, Systems, and Computers in 2003; the International Symposium on Wireless Personal Multimedia Communications (WPMC) in 2006; PacketVideo during 2007–2013; the International Conference on Image Processing during 2008–2011; the International Conference on Visual Communications and Image Processing (VCIP) in 2010; the International Workshop on Quality of Multimedia Experience (QOMEX) during 2010–2012; the International Conference on Multimedia and Expo during 2011–2013; and the International Conference on Communications in 2012. She was the Technical Program Chair of the 1998 Information Theory Workshop in San Diego. She was an Associate Editor of the IEEE COMMUNICATIONS LETTERS (1998–2001), a Guest Editor of the June 2000 special issue of the IEEE JOURNAL ON SELECTED AREAS IN COMMUNICATIONS on "Error-resilient image and video coding," and an Associate Editor of the IEEE SIGNAL PROCESSING LETTERS (2001–2005). She was the Editor-in-Chief (2006–2009) and a Senior Editor (2003–2005 and 2010–2013) of the IEEE JOURNAL ON SELECTED AREAS IN COMMUNICATIONS. She received the ECE Departmental Graduate Teaching Award, a Career Award from the National Science Foundation, a Powell Faculty Fellowship, the 2008 Globecom Best Paper Award, and the 2012 IEEE Conference on Healthcare Informatics, Imaging, and Systems Biology Best Poster Award. She is also a member of Tau Beta Pi and Sigma Xi.

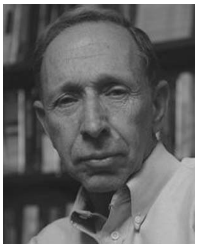

Laurence B. Milstein (S'66–M'68–SM'77–F'85) received the B.E.E. degree from the City College of New York, New York, NY, USA, in 1964 and the M.S. and Ph.D. degrees in electrical engineering from the Polytechnic Institute of Brooklyn, Brooklyn, NY, in 1966 and 1968, respectively.

From 1968 to 1974, he was with the Space and Communications Group, Hughes Aircraft Company. From 1974 to 1976, he was a member of the Department of Electrical and Systems Engineering, Rensselaer Polytechnic Institute, Troy, NY. Since 1976, he has been with the Department of Electrical and Computer Engineering, University of California at San Diego (UCSD), La Jolla, CA, USA, where he is currently the Ericsson Professor of Wireless Communications Access Techniques and a former Department Chairman, working in the area of digital communication theory, with special emphasis on spread-spectrum communication systems. He has been also a consultant to both government and industry in the areas of radar and communications.

Dr. Milstein was the Vice President for Technical Affairs in 1990 and 1991 of the IEEE Communications Society and is a former Chair of the IEEE Fellows Selection Committee. He was an Associate Editor for Communication Theory of the IEEE TRANSACTIONS ON COMMUNICATIONS, an Associate Editor for Book Reviews of the IEEE TRANSACTIONS ON INFORMATION THEORY, an Associate Technical Editor of the IEEE COMMUNICATIONS MAGAZINE, and the Editor-in-Chief of the IEEE JOURNAL ON SELECTED AREAS IN COMMUNICATIONS. He received the 1998 Military Communications Conference Long-Term Technical Achievement Award, an Academic Senate 1999 UCSD Distinguished Teaching Award, an IEEE Third Millennium Medal in 2000, the 2000 IEEE Communication Society Armstrong Technical Achievement Award, and various prize paper awards, including the 2002 Military Communications (MILCOM) Fred Ellersick Award. He also received the IEEE Communications Theory Technical Committee (CTTC) Service Award in 2009, the CTTC Achievement Award in 2012, and the 2015 Chancellor's Award for Excellence in Graduate Teaching.